

Nonlinear model reduction on metric spaces. Application to one-dimensional conservative PDEs in Wasserstein spaces.

V. Ehrlacher, D. Lombardi, O. Mula and F.-X. Vialard

Abstract

We consider the problem of model reduction of parametrized PDEs where the goal is to approximate any function belonging to the set of solutions at a reduced computational cost. For this, the bottom line of most strategies has so far been based on the approximation of the solution set by linear spaces on Hilbert or Banach spaces. This approach can be expected to be successful only when the Kolmogorov width of the set decays fast. While this is the case on certain parabolic or elliptic problems, most transport-dominated problems are expected to present a slow decaying width and require to study nonlinear approximation methods. In this work, we propose to address the reduction problem from the perspective of general metric spaces with a suitably defined notion of distance. We develop and compare two different approaches, one based on barycenters and another one using tangent spaces when the metric space has an additional Riemannian structure. As a consequence of working in metric spaces, both approaches are automatically nonlinear. We give theoretical and numerical evidence of their efficiency to reduce complexity for one-dimensional conservative PDEs where the underlying metric space can be chosen to be the L^2 -Wasserstein space.

1 Introduction

In modern applications of science, industry and numerous other fields, the available time for design and decision-making is becoming shorter, and some tasks are even required to be performed in real time. The process usually involves predictions of the state of complex systems which, in order to be reliable, need to be described by sophisticated models. The predictions are generally the output of inverse or optimal control problems that are formulated on these models and which cannot be solved in real time unless the overall complexity has been appropriately reduced. Our focus lies in the case where the model is given by a Partial Differential Equation (PDE) that depends on certain parameters. In this setting, the routines for prediction require to evaluate solutions of the PDE on a large set of dynamically updated parameters. This motivates the search for accurate and online methods to approximate the solutions at a reduced computational cost. This task, usually known as *reduced modelling* or *model order reduction*, can be summarized as follows.

Let Ω be a domain of \mathbb{R}^d for a given dimension $d \geq 1$ and let (V, d) be a metric space of functions defined over Ω , with metric d . The main goal of model reduction is to approximate as accurately and quickly as possible the solution $u(z) \in V$ of a problem of the form

$$\mathcal{P}(u(z), z) = 0 \tag{1.1}$$

for many different values of a vector $z = (z_1, \dots, z_p)$ in a certain range $Z \subset \mathbb{R}^p$. In the above formula, \mathcal{P} is a differential or integro-differential operator parametrized by z , and we assume that for each $z \in Z$ there exists a unique solution $u(z) \in V$ to problem (1.1). The set of all solutions is defined as

$$\mathcal{M} := \{u(z) : z \in Z\} \subset V, \tag{1.2}$$

and is often referred to as the solution manifold with some abuse of terminology¹.

In the context of model reduction, V is traditionally chosen to be a Banach or a Hilbert space with the metric given by its norm denoted by $\|\cdot\|$. However, certain problems can only be defined over metric spaces V . For instance, it has been proven for numerous nonlinear dissipative evolution equations that they can be formulated in the form of Wasserstein gradient flows. To name a few

¹This set of solutions may not be a differentiable manifold in infinite dimensions.

see [28] for Hele-Shaw flows, [29] for quantum problems, [51] for porous media flows, [37] for Fokker-Planck equations and [61, 12] for Keller-Segel models in chemotaxis. Other examples involving metric spaces that are not necessarily related to gradient flows are [13] for the Camassa-Holm equation, [17] for the Hunter-Saxton equation. Such examples can often be interpreted as a geodesic flow on a group of diffeomorphisms and can thus be encoded as Hamiltonian flows. Therefore, extending the notion of model reduction in Banach/Hilbert spaces to more general metric spaces could enlarge the scope of problems that can potentially be addressed.

To develop further on the potential interest brought by nonlinear model reduction on metric spaces, let us briefly recall the classical lines followed for model reduction on Banach/Hilbert spaces. Assume for now that V is a Banach space. Most methods are typically based on determining a “good” n -dimensional subspace $V_n = \text{span}\{v_1, \dots, v_n\} \subset V$ that yields efficient approximations of $u(z)$ in V_n of the form

$$u_n(z) := \sum_{i=1}^n c_i(z)v_i \quad (1.3)$$

for some coefficients $c_1(z), \dots, c_n(z) \in \mathbb{R}$. This approach is the backbone of most existing methods among which stand the reduced basis method ([34, 54]), the empirical interpolation method and its generalized version (G-EIM, [7, 32, 43, 44]), Principal Component Analysis (PCA, see [8, Chapter 1]), polynomial-based methods like [22, 23] or low-rank methods ([38]).

The approximation quality of the obtained subspace V_n is either measured through the worst case error

$$e_{\text{wc}}(\mathcal{M}, V, V_n) := \sup_{z \in Z} \inf_{w_n \in V_n} d(u(z), w_n), \quad (1.4)$$

or the average error

$$e_{\text{av}}(\mathcal{M}, V, V_n) := \left(\int_{z \in Z} \inf_{w_n \in V_n} d^2(u(z), w_n) d\mu(z) \right)^{1/2}, \quad (1.5)$$

where μ is a probability measure on Z , given a priori and from which the parameters are sampled.

The reduction method is considered efficient if $e_{\text{wc}}(\mathcal{M}, V, V_n)$ (or $e_{\text{av}}(\mathcal{M}, V, V_n)$) decays rapidly to 0 as n goes to ∞ . There is sound evidence of efficiency only in the case of certain elliptic and parabolic PDEs. More precisely, it has been shown in [21] that for this type of equations, under suitable assumptions, the L^∞ Kolmogorov width defined as

$$d_n(\mathcal{M}, V) := \inf_{\substack{V_n \subset V, \\ \dim V_n = n}} e_{\text{wc}}(\mathcal{M}, V, V_n) \quad (1.6)$$

and the L^2 Kolmogorov width

$$\delta_n(\mathcal{M}, V) := \inf_{\substack{V_n \subset V, \\ \dim V_n = n}} e_{\text{av}}(\mathcal{M}, V, V_n) \quad (1.7)$$

decay exponentially or polynomially with high exponent as n grows. In the context of model reduction, this quantity gives the best possible performance that one can achieve when approximating \mathcal{M} with n -dimensional linear spaces.

Optimal linear subspaces $V_n \subset V$ of dimension n which realize the infimum of (1.6) cannot be computed in practice in general. However, it has been shown that greedy algorithms can be used to build sequences of linear spaces $(V_n)_{n \geq 1}$ whose approximation error $e_{\text{wc}}(\mathcal{M}, V_n)$ decay at a comparable rate as the Kolmogorov n -width $d_n(\mathcal{M}, V)$. These algorithms are the backbone of the so-called Reduced Basis method [10]. In the case of (1.7), the optimal subspaces for which the minimum is attained are obtained using the PCA (or POD) method (also called POD).

In this paper, our goal is to extend the above notion of model reduction to more general metric spaces in view of the following facts. First of all, in the context of Banach or Hilbert spaces, linear methods are unfortunately not well suited for hyperbolic problems. Among others, this is due to the transport of shock discontinuities whose locations may vary together with the parameters. To illustrate this claim, we show in section 3.1 that the L^∞ Kolmogorov width of a simple pure transport problem decays very slowly at a rate $n^{-1/2}$ if $V = L^2$ (similar examples can be found in [59, 11]). The same type of result has recently been derived for wave propagation problems in [31]. These results highlight that linear methods of the type (1.3) are not expected to provide a fast decay in numerous transport dominated problems, and may be highly suboptimal in terms of the trade off between accuracy and numerical complexity. For these classes of problems, an efficient strategy for model

reduction requires to look for *nonlinear methods* that capture the geometry of \mathcal{M} in a finer manner than linear spaces. In addition to the idea of searching for nonlinear methods, it may be beneficial to move from the classical Banach/Hilbert metric framework to more general metric spaces in order to better quantify the ability to capture specific important features like translations or shifts. Finally, as already brought up, this broader setting enlarges the scope of problems that can be treated.

We next describe the state of the art methods proposed to go beyond the linear case and to address hyperbolic problems. Then, we summarize the contribution and the organization of this paper.

1.1 State of the art

Works on adaptivity. Several works try to circumvent the poor representation given by linear spaces by building local spaces. In [16] a strategy inspired by the mesh h -refinement is proposed. In [6, 5] a construction of linear subspaces is proposed, based on a k -means clustering that groups together similar snapshots of the solution. A similar approach is presented in [52] to overcome some shortcomings of the DEIM approach. In the two recent preprints [41, 30], the subspaces to be used for model reduction are identified by using autoencoders and neural networks.

Stabilization strategies. Advection dominated problems tend to show potential instabilities when reduced-order integrators are built. In [42, 57] an online stabilization is proposed. A form of stabilization based on an L^1 minimisation problem is proposed in [1].

Reduced-order modeling from a geometrical point of view. Several works in the literature propose to transform the snapshots by making a Lie group acting on them. In [46] the authors propose a method to get rid of continuous symmetries in parametric dynamical systems whose dynamics is invariant under continuous group action². A similar approach was proposed in [50].

Conversely to transporting the snapshots, dynamical bases approaches are defined in which the subspace used to approximate the solution evolves in time. An example of such a method is the Dynamically Orthogonal (DO) decomposition (detailed in [39, 40, 47, 25]). We also cite [4] and a recent extension [45], which have focused on model reduction over the Grassman manifold.

In the context of Hamiltonian systems, [2, 33] introduce a reduced-order framework that preserves the symplectic structure of the dynamical system.

Non-linear transformations. In [59, 60], a transformed snapshot interpolation method is introduced, aiming at finding a set of non-linear transformations such that the approximation of the transformed snapshots by a linear combination of modes is efficient. In [48], which addresses compressible fluid-dynamics, the set of the snapshots is transported into a reference configuration by a displacement field which is identified through a polynomial expansion. In [36], the authors propose a non-linear model reduction strategy based on optimal transport and the reduction of optimal transport maps. Another strategy based on non-linear transformations was proposed in [14] to deal with hyperbolic problems with applications to transonic flows around airfoils. Finally, the recent work [15] introduces a general framework to look for reference configurations and for transformations depending upon few parameters in order to deal with advection dominated problems.

1.2 Contribution and organization of the paper

The main contribution of this work is to develop the idea of reduced modeling in metric spaces. For this:

- We give theoretical evidence on two simple PDEs (pure transport and Burger’s equation in 1D) that it is beneficial to do model reduction on metric spaces rather than on more classical Banach spaces.
- We develop two model reduction strategies on general metric spaces, one based on tangent spaces, the second one based on barycenters.

Our approach is, to the best of our knowledge, novel in the field of reduced modelling. The first approach is however related to the so-called tangent PCA, which has drawn significant interest in numerous fields like pattern recognition, shape analysis, medical imaging, computer vision [26, 56]. More recently, it has also been used in statistics [35] and machine learning to study families of histograms and probability densities [18]. Our second approach based on barycenters is entirely novel to the best of our knowledge, and it could be used as an alternative to tPCA in other applications apart from model reduction.

²On the KdV equations these symmetries were studied analytically in [27]

As a support for our numerical tests, we will consider the model reduction of one-dimensional conservative PDEs in the L^2 -Wasserstein metric. Time will be seen as one of the parameters. The precise setting and notation is the following. For a given open interval $\Omega \subset \mathbb{R}$ and a given final time $T > 0$, we consider a 1d conservative PDE that depends on $\tilde{p} \in \mathbb{N}^*$ parameters which belong to a compact set $Y \subset \mathbb{R}^{\tilde{p}}$. For a given $y \in Y$, $u_y : [0, T] \times \Omega \rightarrow \mathbb{R}$ is the solution to

$$\partial_t u_y(t, x) - \partial_x F(u_y(t, x); y, t) = 0, \quad \forall (t, x) \in [0, T] \times \Omega, \quad (1.8)$$

with appropriate initial and boundary conditions. We assume that $F(\cdot; y, t)$ is a real-valued mapping defined on a set of functions defined on Ω so that the solution to (1.8) is well-defined and

$$u_y(t, \cdot) \in \mathcal{P}_2(\Omega), \quad \forall (t, y) \in Z := [0, T] \times Y,$$

where $\mathcal{P}_2(\Omega)$ denotes the set of probability measures on Ω with finite second-order moments. Since time is an additional parameter, our parameter set is

$$Z := [0, T] \times Y \subset \mathbb{R}^p, \quad p := \tilde{p} + 1$$

thus the solution set is

$$\mathcal{M} := \{u(z) = u_y(t, \cdot) \in \mathcal{P}_2(\Omega) : z = (t, y) \in Z\} \subset \mathcal{P}_2(\Omega).$$

The paper is organized as follows: We begin by recalling in Section 2 basic notions on metric spaces, and more specifically on the L^2 -Wasserstein space in one dimension. We then highlight in Section 3 the interest of doing model reduction of conservative PDEs in metric spaces. For two simple PDEs (a pure transport equation and an inviscid Burger's equation in 1D), we prove theoretically that this point of view yields better approximation properties than classical linear methods on Banach spaces. In Section 4, we describe the two numerical methods (tPCA and gBar) that we propose for model reduction in general metric spaces. We also make the different steps of the algorithms explicit in the particular case of the L^2 Wasserstein space in 1D. Finally, Section 6 gives numerical evidence of the performance of the two algorithms on four different problems: an inviscous and viscous Burger's equation, a Camassa-Holm equation and a Korteweg-de-Vries (KdV) equation. The results illustrate the ability of the proposed methods to capture transport phenomena. The KdV problem shows some limitations of the methodology in terms of capturing the fusion and separation of peakons and motivates our final section 7, where we list possible extensions to address not only this issue, but also to treat more general multi-dimensional and non-conservative problems.

Connections with other fields of research: In the field of machine learning and statistics, there have been several con

The present work shares a point of contact with current developments made in the fields of statistic and machine learning

The model reduction of conservative PDEs in the L^2 -Wasserstein metric

2 Metric spaces and Wasserstein space

Since in our numerical examples we focus on the model reduction of parametric one-dimensional conservative PDEs in the L^2 -Wasserstein space, we start this section by recalling some basic properties of this space. We next recall the definition of exponential and logarithmic maps on general Riemannian manifolds, and then detail their expression in the case of the 1D Wasserstein space. Finally, we introduce the notion of barycenters on general metric spaces.

2.1 Definition of the L^2 -Wasserstein space in one dimension

Let $\Omega = [x_{\min}, x_{\max}] \subset \mathbb{R}$, with $-\infty \leq x_{\min} < x_{\max} \leq \infty$ be the domain of interest. Let $\mathcal{P}_2(\Omega)$ denote the set of probability measures on Ω with finite second-order moments. For all $u \in \mathcal{P}_2(\Omega)$, we denote by

$$\text{cdf}_u : \begin{cases} \Omega & \rightarrow \\ x & \mapsto \text{cdf}_u(x) := \int_{x_{\min}}^x u(x') dx' \end{cases} \quad (2.1)$$

its cumulative distribution function (cdf), and by

$$\text{icdf}_u : \begin{cases} [0, 1] & \rightarrow \\ s & \mapsto \text{cdf}_u^{-1}(s) := \inf\{x \in \Omega, \text{cdf}_u(x) > s\} \end{cases} \quad (2.2)$$

the generalized inverse of the cdf (icdf). The L^2 -Wasserstein distance is defined by

$$W_2(u, v) := \inf_{\pi \in \Pi(u, v)} \left(\int_{\Omega \times \Omega} (x - y)^2 d\pi(x, y) \right)^{1/2}, \quad \forall (u, v) \in \mathcal{P}_2(\Omega) \times \mathcal{P}_2(\Omega),$$

where $\Pi(u, v)$ is the set of probability measures on $\Omega \times \Omega$ with marginals u and v . In the particular case of one dimensional marginal domains, it can be equivalently expressed using the inverse cumulative distribution functions as

$$W_2(u, v) = \|\text{icdf}_u - \text{icdf}_v\|_{L^2([0,1])}. \quad (2.3)$$

The space $\mathcal{P}_2(\Omega)$ endowed with the distance W_2 is a metric space, usually called L^2 -Wasserstein space (see [58] for more details).

2.2 Exponential and logarithmic maps

Let (V, d) be a metric space where V is a Riemannian manifold. For any $w \in V$, we denote by $T_w V$ the tangent space to V at point w . Then, there exists a subset $\mathcal{O}_w \subset T_w V$ such that the exponential map $\text{Exp}_w : \mathcal{O}_w \rightarrow V$ can be defined and is a diffeomorphism onto its image. The logarithmic map $\text{Log}_w : \text{Exp}_w(\mathcal{O}_w) \rightarrow \mathcal{O}_w$ is then defined as the generalized inverse of Exp_w .

In the case when $(V, d) = (\mathcal{P}_2(\Omega), W_2)$, the exponential and logarithmic maps have a particular simple form which we explain next. We can take advantage of the fact that, after composition with the nonlinear map $\mathcal{P}_2(\Omega) \ni u \mapsto \text{icdf}_u \in L^2([0,1])$, the space $(\mathcal{P}_2(\Omega), W_2)$ is isometric to $(\mathcal{I}, \|\cdot\|_{L^2([0,1])})$, where

$$\mathcal{I} := \{\text{icdf}_u, u \in \mathcal{P}_2(\Omega)\} \quad (2.4)$$

is a convex subset of $L^2([0,1])$. The following well-known result then holds.

Theorem 2.1. *The map $\text{icdf} : \mathcal{P}_2(\Omega) \rightarrow \mathcal{I}$ defined by $\text{icdf}(u) = \text{icdf}_u$ is an (homeomorphism) isometry between $(\mathcal{P}_2(\Omega), W_2)$ and $(\mathcal{I}, \|\cdot\|_{L^2([0,1])})$.*

The fact that the map icdf is an isometry is actually a consequence of (2.3). Note that the inverse of icdf can be computed as

$$\text{icdf}^{-1}(f) = \frac{d}{dx}[f^{-1}], \quad \forall f \in \mathcal{I}.$$

For all $f_0 \in \mathcal{I}$, we introduce

$$\mathcal{K}_{f_0} = \{f \in L^2([0,1]; \Omega) : f_0 + f \in \mathcal{I}\}. \quad (2.5)$$

which is a closed convex subset of $T_{f_0} \mathcal{I}$.

For a given element $w \in \mathcal{P}_2(\Omega)$, using a slight abuse of notation, the exponential map can be advantageously defined on $\mathcal{K}_{\text{icdf}_w}$. Indeed, the definition domain $\mathcal{O}_w \subset T_w \mathcal{P}_2(\Omega)$ of Exp_w is isomorphic to $\mathcal{K}_{\text{icdf}_w}$. Using another slight abuse of notation, we will denote in the sequel $\mathcal{O}_w := \mathcal{K}_{\text{icdf}_w}$. This leads us to the following definition of the exponential and logarithmic maps.

Definition 2.2. Let $w \in \mathcal{P}_2(\Omega)$ be a probability measure. The exponential map $\text{Exp}_w : \mathcal{O}_w \rightarrow \mathcal{P}_2(\Omega)$ is defined as

$$\text{Exp}_w(f) = \text{icdf}^{-1}(\text{icdf}_w + f), \quad \forall f \in \mathcal{O}_w. \quad (2.6)$$

It is surjective and we can define its inverse $\text{Log}_w : \mathcal{P}_2(\Omega) \rightarrow \mathcal{O}_w$ as

$$\text{Log}_w(u) = \text{icdf}_u - \text{icdf}_w, \quad \forall u \in \mathcal{P}_2(\Omega). \quad (2.7)$$

As a consequence of Theorem 2.1, the following result holds.

Corollary 2.3. *The exponential map Exp_w is an isometric homeomorphism between \mathcal{O}_w and $\mathcal{P}_2(\Omega)$ with inverse Log_w and it holds that*

$$W_2(u, v) = \|\text{Log}_w(u) - \text{Log}_w(v)\|_{L^2([0,1])}, \quad \forall (u, v) \in \mathcal{P}_2(\Omega) \times \mathcal{P}_2(\Omega).$$

For the proofs of Theorems 2.3 and 2.1, we refer to [9]. We next give two simple common examples of logarithmic and exponential maps:

- **Dirac masses:** Let $\Omega = \mathbb{R}$ and consider the family of Dirac masses $\{\delta_x : x \in \mathbb{R}\} \subset \mathcal{P}_2(\Omega)$. For any $x \in \mathbb{R}$ and $s \in (0, 1)$, $\text{icdf}_{\delta_x}(s) = x$, thus $W_2(\delta_{x_1}, \delta_{x_2}) = |x_1 - x_2|$ for any $(x_1, x_2) \in \mathbb{R} \times \mathbb{R}$. From (2.7), for all $s \in (0, 1)$, $\text{Log}_{\delta_{x_2}}(\delta_{x_1})(s) = x_1 - x_2$.

- **Translations and rescaling:** Let $w \in \mathcal{P}_2(\mathbb{R})$ with density p_w and, for $(a, b) \in (0, \infty) \times \mathbb{R}$, let $w^{(a,b)}$ be the probability measure with density given by

$$p^{(a,b)}(x) = p_w\left(\frac{x-b}{a}\right),$$

In other words, $\{w^{(a,b)} : (a, b) \in (0, \infty) \times \mathbb{R}\}$ is the family of shifted and rescaled probabilities around w . Then,

$$\text{cdf}_{w^{(a,b)}}(x) := a \text{cdf}_w(ax + b), \quad \forall x \in \mathbb{R}, \quad \text{icdf}_{w^{(a,b)}}(s) := \frac{1}{a} \text{cdf}_w\left(\frac{s}{a}\right) - b, \quad \forall s \in [0, 1]. \quad (2.8)$$

2.3 Barycenters

We next introduce the notion of barycenters in a general metric space (V, d) . Let $n \in \mathbb{N}^*$ and let

$$\Sigma_n := \left\{ (\lambda_1, \dots, \lambda_n) \in [0, 1]^n, \quad \sum_{i=1}^n \lambda_i = 1 \right\}$$

be the set of barycentric weights. For any $U_n = (u_i)_{1 \leq i \leq n} \in V^n$ and barycentric weights $\Lambda_n = (\lambda_i)_{1 \leq i \leq n} \in \Sigma_n$, an associated barycenter is an element of V which minimizes

$$\inf_{v \in V} \sum_{i=1}^n \lambda_i d(v, u_i)^2. \quad (2.9)$$

In full generality, minimizers to (2.9) may not be unique. In the following, we call $\text{Bar}(U_n, \Lambda_n)$ the set of minimizers to (2.9), which is the set of barycenters of U_n with barycentric weights Λ_n .

It will be useful to introduce the notion of *optimal barycenter* of an element $u \in V$ for a given family $U_n \in V^n$. The set of barycenters with respect to U_n is

$$\mathcal{B}_n(U_n) := \bigcup_{\Lambda_n \in \Sigma_n} \text{Bar}(U_n, \Lambda_n)$$

and an optimal barycenter of the function $u \in V$ with respect to the set U_n is a minimizer of

$$\min_{b \in \mathcal{B}_n(U_n)} d(u, b)^2. \quad (2.10)$$

In other words, a minimizer to (2.10) is the projection of u on the set of barycenters $\mathcal{B}_n(U_n)$.

We next present some properties of barycenters in the Wasserstein space $(V, d) = (\mathcal{P}_2(\Omega), W_2)$ which will be relevant for our developments (see [3] for further details). The first property is that problem (2.9) has a unique solution, that is, for a family of probability measures $U_n = (u_i)_{1 \leq i \leq n} \in \mathcal{P}_2(\Omega)^n$ and barycentric weights $\Lambda_n = (\lambda_i)_{1 \leq i \leq n} \in \Sigma_n$, there exists a unique minimizer to

$$\min_{v \in \mathcal{P}_2(\Omega)} \sum_{i=1}^n \lambda_i W_2(v, u_i)^2, \quad (2.11)$$

which is denoted by $\text{Bar}(U_n, \Lambda_n)$. In addition, the barycenter can be easily characterized in terms of its inverse cumulative distribution function since (2.11) implies that

$$\text{icdf}_{\text{Bar}(U_n, \Lambda_n)} = \arg \min_{f \in L^2([0,1])} \sum_{i=1}^n \lambda_i \| \text{icdf}_{u_i} - f \|_{L^2([0,1])}^2, \quad (2.12)$$

which yields

$$\text{icdf}_{\text{Bar}(U_n, \Lambda_n)} = \sum_{i=1}^n \lambda_i \text{icdf}_{u_i}. \quad (2.13)$$

The *optimal barycenter* of a function $u \in \mathcal{P}_2(\Omega)$ for a given set of functions U_n is unique. We denote it $b(u, U_n)$ and it can be easily characterized in terms of its inverse cumulative distribution function. Indeed, the minimization problem (2.10) reads in this case

$$\min_{b \in \mathcal{B}_n(U_n)} W_2(u, b)^2$$

and it has a unique minimizer $b(u, U_n)$. An alternative formulation of the optimal barycenter is by finding first the optimal weights

$$\Lambda_n^{\text{opt}} = \arg \min_{\Lambda_n \in \Sigma_n} W_2^2(u, \text{Bar}(U_n, \Lambda_n)). \quad (2.14)$$

The optimal barycenter is then

$$b(u, U_n) = \text{Bar}(U_n, \Lambda_n^{\text{opt}}).$$

Note that for all $\Lambda_n \in \Sigma_n$ and all $w \in \mathcal{P}_2(\Omega)$,

$$\begin{aligned} W_2^2(u, \text{Bar}(U_n, \Lambda_n)) &= \left\| \text{icdf}_u - \sum_{i=1}^n \lambda_i \text{icdf}_{u_i} \right\|_{L^2([0,1])}^2 \\ &= \left\| \text{Log}_w(u) - \sum_{i=1}^n \lambda_i \text{Log}_w(u_i) \right\|_{L^2([0,1])}^2 \end{aligned}$$

so the computation of the optimal weights Λ_n^{opt} in problem (2.14) is a simple cone quadratic optimization problem.

For a given $w \in \mathcal{P}_2(\Omega)$, denoting

$$\mathbb{T}_n = \text{Log}_w(U_n) = \{\text{Log}_w(u_1), \dots, \text{Log}_w(u_n)\}$$

the logarithmic image of U_n and $\text{Conv}(\mathbb{T}_n)$ the convex hull of \mathbb{T}_n , we see that $\text{Log}_w(b(u, U_n))$ is the projection of $\text{Log}_w(u)$ onto $\text{Conv}(\mathbb{T}_n)$, namely

$$\text{Log}_w(b(u, U_n)) = \arg \min_{f \in \text{Conv}(\mathbb{T}_n)} \|\text{Log}_w(u) - f\|_{L^2([0,1])}^2. \quad (2.15)$$

3 Kolmogorov n -widths for two simple conservative PDEs

In the sequel, \mathcal{M} is the set of solutions of a parametric conservative PDE in one dimension. Instead of working in the usual Banach/Hilbert setting, we assume that $\mathcal{M} \subset \mathcal{P}_2(\Omega)$. We denote

$$\mathcal{T} := \text{Log}_w(\mathcal{M}) \subset L^2([0, 1]),$$

the image of \mathcal{M} by the logarithmic map Log_w , where w is an element of $\mathcal{P}_2(\Omega)$ which will be fixed later on.

To illustrate the interest of working with this metric, we show in a pure transport equation and in an inviscid Burger's equation that the decay rate of Kolmogorov widths $d_n(\mathcal{T}, L^2([0, 1]))$ and $\delta_n(\mathcal{T}, L^2([0, 1]))$ at a faster rate than the widths $d_n(\mathcal{M}, L^2(\Omega))$ and $\delta_n(\mathcal{M}, L^2(\Omega))$ of the original set of solutions \mathcal{M} . This shows that it is convenient to transform the original data \mathcal{M} to \mathcal{T} by the nonlinear logarithmic mapping before performing the dimensionality reduction. Indeed, if $d_n(\mathcal{T}, L^2([0, 1]))$ (or $\delta_n(\mathcal{T}, L^2([0, 1]))$) decay fast, then there exist spaces $V_n \subset L^2([0, 1])$ such that

$$e_{\text{wc}}(\mathcal{T}, L^2([0, 1]), V_n) = \sup_{f \in \mathcal{T}} \|f - P_{V_n} f\|_{L^2([0,1])}$$

decays fast as $n \rightarrow \infty$. Thus if for all $f \in \mathcal{T}$ the projections $P_{V_n} f \in \mathcal{O}_w$, then their exponential map is well defined and we can approximate any $u \in \mathcal{M}$ with $\text{Exp}_w(P_{V_n} \text{Log}_w(u))$. Due to the isometric properties of Exp_w (see corollary 2.3), the approximation error of \mathcal{M} is

$$e_{\text{wc}}(\mathcal{M}, W_2, V_n) := \sup_{u \in \mathcal{M}} W_2(u, \text{Exp}_w(P_{V_n} \text{Log}_w(u))) = e_{\text{wc}}(\mathcal{T}, L^2([0, 1]), V_n).$$

Thus the existence of linear spaces $(V_n)_{n \geq 1}$ in $L^2([0, 1])$ with good approximation properties for \mathcal{T} automatically yields good low rank nonlinear approximations for \mathcal{M} (provided that the exponential map is well defined).

Note that this idea can be generalized to general metric spaces (V, d) provided that the following hypothesis is satisfied.

Hypothesis 3.1. *There exists an inner product g_w on $T_w V$ at a given point $w \in V$ such that $\text{Exp}_w : \mathcal{O}_w \rightarrow V$ is an homeomorphism between \mathcal{O}_w and V with inverse Log_w and we have an isometric equivalence, that is, there exist constants $0 < \underline{c} \leq \bar{c}$ such that*

$$\underline{c} d(u, v) \leq g_w(\text{Log}_w(u) - \text{Log}_w(v), \text{Log}_w(u) - \text{Log}_w(v)) \leq \bar{c} d(u, v), \quad \forall (u, v) \in V \times V.$$

3.1 A pure transport problem

We consider here a prototypical example similar to the one given in [11] (see also [59, 31] for other examples). Consider the univariate transport equation

$$\partial_t u_y(t, x) + y \partial_x u_y(t, x) = 0, \quad x \in \mathbb{R}, t \geq 0,$$

with initial value $u_0(x) = \mathbb{1}_{[-1, 0]}$, and parameter $y \in Y := [0, 1]$. Note that this is a conservative problem since for all $t \geq 0$, $\int_{\mathbb{R}} u(t, x) dx = 1$. We consider the parametrized family of solutions at time $t = 1$ restricted to $x \in \Omega := [-1, 1]$, that is

$$\mathcal{M} = \{u(z) = u_y(t = 1, \cdot) := \mathbb{1}_{[y-1, y]} : z = (t, y) \in \{1\} \times [0, 1]\}.$$

Note that here t is fixed so it is not a varying parameter. We have kept it in the notation in order to remain consistent with the notation of the introduction.

Since $\mathcal{M} \subset \mathcal{P}_2([-1, 1])$, we can define

$$\mathcal{T} = \{\text{Log}_w(u(z)), z \in Z\} = \left\{ \text{icdf}_{\mathbb{1}_{[y-1, y]}} - \text{icdf}_w, y \in [0, 1] \right\},$$

where w is chosen as $\mathbb{1}_{[y_0-1, y_0]}$ for some $y_0 \in [0, 1]$.

In the following theorem, we prove two extreme convergence results. On the one hand we prove that $d_n(\mathcal{T}, L^2([0, 1])) = 0$ for $n > 1$. On the other hand, we show that $d_n(\mathcal{M}, L^2(\Omega))$ cannot decay faster than the rate $n^{-1/2}$. We derive the result in the L^2 metric since it is very commonly considered but a similar reasoning would give a rate of n^{-1} in L^1 (see, e.g., [59]). This rigorously proves that standard linear methods cannot be competitive for reducing this type of problems and that shifting the problem from \mathcal{M} to \mathcal{T} dramatically helps in reducing the complexity in the pure transport case.

Theorem 3.2. *There exists a constant $c > 0$ such that for all $n \in \mathbb{N}^*$,*

$$d_n(\mathcal{M}, L^2(\Omega)) \geq \delta_n(\mathcal{M}, L^2(\Omega)) \geq cn^{-1/2}. \quad (3.1)$$

In addition, for $n > 1$, $d_n(\mathcal{T}, L^2([0, 1])) = 0$.

Proof. We first prove that $d_n(\mathcal{T}, L^2([0, 1])) = 0$ for $n > 1$. Since for every $y \in [0, 1]$, $\mathbb{1}_{[y-1, y]} = \mathbb{1}_{[y_0-1, y_0]}(x - y + y_0)$, using (2.8), it holds that

$$\text{icdf}_{\mathbb{1}_{[y-1, y]}}(s) = \text{icdf}_{\mathbb{1}_{[y_0-1, y_0]}}(s) - y_0 + y, \quad \forall s \in [0, 1],$$

and for all $s \in [0, 1]$,

$$\text{Log}_w(\mathbb{1}_{[y-1, y]})(s) = \text{icdf}_{\mathbb{1}_{[y-1, y]}}^{-1}(s) - \text{icdf}_{\mathbb{1}_{[y_0-1, y_0]}}^{-1}(s) = y - y_0.$$

As a consequence, the set \mathcal{T} is contained in the one-dimensional space of constant functions defined on $(0, 1)$ and $d_n(\mathcal{T}, L^2([0, 1])) = 0$ for all $n > 1$.

We next prove (3.1). Let $n \in \mathbb{N}^*$. The inequality $d_n(\mathcal{M}, L^2(\Omega)) \geq \delta_n(\mathcal{M}, L^2(\Omega))$ is a direct consequence of the fact that for all finite-dimensional subspace $V_n \subset L^2(\Omega)$ of dimension n ,

$$\sup_{z \in Z} \|u(z) - P_{V_n} u(z)\|_{L^2(\Omega)} \geq \left(\int_Z \|u(z) - P_{V_n} u(z)\|_{L^2(\Omega)}^2 dz \right)^{1/2}.$$

Thus, we only have to prove that there exists a constant $c > 0$ such that for all $n \in \mathbb{N}^*$,

$$\delta_n(\mathcal{M}, L^2(\Omega)) \geq cn^{-1/2}.$$

To obtain this result, we express $\delta_n(\mathcal{M}, L^2(\Omega))$ as a function of the eigenvalues of the so-called correlation operator $K : L^2(\Omega) \rightarrow L^2(\Omega)$ which is defined as follows:

$$\forall v \in L^2(\Omega), \quad (Kv)(x) = \int_{\Omega} \kappa(x, x') v(x') dx',$$

where $\kappa(x, x') := \int_{z \in Z} u(z)(x) u(z)(x') dy$. Since $u(z) = \mathbb{1}_{[z-1, z]}$, it holds that

$$\kappa(x, x') = \begin{cases} \max(0, 1 - |x - x'|) & \text{if } (x, x') \in [-1, 0] \times [0, 1] \cup [0, 1] \times [-1, 0], \\ 1 - \max(x, x') & \text{if } (x, x') \in [0, 1] \times [0, 1], \\ 1 - \max(|x|, |x'|) & \text{if } (x, x') \in [-1, 0] \times [-1, 0], \end{cases}$$

The function κ is continuous and piecewise affine on $\Omega \times \Omega$, and $\kappa = 0$ on $\partial(\Omega \times \Omega)$. We denote by $e_{k,k'}(x) := \frac{1}{2}e^{i(kx+k'x')}$ for all $k, k' \in \mathbb{Z}$, so the Fourier coefficient of κ associated to the (k, k') Fourier mode is defined by

$$\alpha_{k,k'} := \langle \kappa, e_{k,k'} \rangle.$$

It can be easily checked that there exists a constant $C > 0$ such that for all $k, k' \in \mathbb{Z}$,

$$|\alpha_{k,k'}| \geq C \frac{1}{(|k| + |k'|)^2}. \quad (3.2)$$

The correlation operator K is a compact self-adjoint non-negative operator on $L^2(\Omega)$. Thus, there exists an orthonormal family $(f_k)_{k \in \mathbb{N}^*}$ and a non-increasing sequence of non-negative real numbers $(\sigma_k)_{k \in \mathbb{N}^*}$ going to 0 as k goes to $+\infty$ such that

$$Kf_k = \sigma_k f_k, \quad \forall k \in \mathbb{N}^*.$$

The scalars $\sigma_1 \geq \sigma_2 \geq \dots \geq 0$ are the eigenvalues of the operator K , and it holds that

$$\delta_n(\mathcal{M}, L^2(\Omega)) = \sqrt{\sum_{k \geq n+1} \sigma_k}.$$

The n^{th} eigenvalue σ_n can be identified through the Max-Min formulas

$$\sigma_n = \max_{\substack{V_n \subset L^2(\Omega) \\ \dim V_n = n}} \min_{\substack{v_n \in V_n \\ \|v_n\|_{L^2(\Omega)} = 1}} \langle v_n, K v_n \rangle_{L^2(\Omega)}.$$

We define $V_n := \text{Span} \left\{ \frac{1}{\sqrt{2}} e^{ik\cdot}, \quad k \in \mathbb{Z}, |k| \leq n \right\}$. Using (3.2), it can easily be checked that there exists a constant $c' > 0$ such that for all $n \in \mathbb{N}^*$,

$$\min_{\substack{v_n \in V_n \\ \|v_n\|_{L^2(\Omega)} = 1}} \langle v_n, K v_n \rangle_{L^2(-1,1)} = \min_{\substack{(\gamma_k)_{|k| \leq n} \in \mathbb{C}^{2n+1} \\ \sum_{|k| \leq n} |\gamma_k|^2 = 1}} \sum_{|k|, |k'| \leq n} \alpha_{k,k'} \gamma_k \overline{\gamma_{k'}} \geq c' \frac{1}{n^2}.$$

Thus, for all $n \in \mathbb{N}^*$, $\sigma_n \geq c'n^{-2}$ and there exists a constant $c > 0$ such that for all $n \in \mathbb{N}^*$,

$$\delta_n(\mathcal{M}, L^2(\Omega)) = \sqrt{\sum_{k \geq n+1} \sigma_k} \geq cn^{-1/2}.$$

□

3.2 An inviscid Burger's equation

In this section, we consider a simple inviscid Burger's equation. We study a simple though representative example where we prove that the Kolmogorov n -width of \mathcal{T} decays faster as n increases than the Kolmogorov n -width of \mathcal{M} .

Let $Y = [1/2, 3]$, and for all $y \in Y$, let us consider the inviscid Burger's equation for $(t, x) \in [0, T] \times \Omega = [0, 5] \times [-1, 4]$,

$$\partial_t u_y + \frac{1}{2} \partial_x (u_y^2) = 0, \quad u_y(t=0, x) = \begin{cases} 0, & -1 \leq x < 0 \\ y, & 0 \leq x < \frac{1}{y} \\ 0, & \frac{1}{y} \leq x \leq 4, \end{cases} \quad (3.3)$$

with periodic boundary conditions on Ω .

Problem (6.1) has a unique entropic solution which reads as follows. For $0 < t < 2/y$, a wave composed of a shock front and a rarefaction wave propagates from left to right and

$$u_y(t, x) = \begin{cases} 0, & -1 \leq x < 0 \\ \frac{x}{t}, & 0 \leq x < yt \\ y, & yt \leq x \leq \frac{1}{y} + \frac{yt}{2}, \\ 0, & \frac{1}{y} + \frac{yt}{2} < x \leq 4 \end{cases}, \quad 0 < t < 2/y^2. \quad (3.4)$$

The rarefaction wave reaches the front at $t = 2/y^2$ so that for $t \geq 2/y^2$,

$$u_y(t, x) = \begin{cases} 0, & -1 \leq x < 0 \\ \frac{x}{t}, & 0 \leq x \leq \sqrt{2t}, \\ 0, & x > \sqrt{2t} \end{cases} \quad \forall t \geq 2/y^2 \quad (3.5)$$

The cumulative distribution function $\text{cdf}_{u_y(t, \cdot)} : \Omega \rightarrow [0, 1]$ of $u(t, \cdot, y)$ is equal to

$$\text{cdf}_{u_y(t, \cdot)}(x) = \begin{cases} 0, & -1 \leq x < 0 \\ \frac{x^2}{2t}, & 0 \leq x < yt \\ yx - \frac{y^2 t}{2}, & yt \leq x \leq \frac{1}{y} + \frac{yt}{2}, \\ 1, & \frac{1}{y} + \frac{yt}{2} < x \leq 4 \end{cases} \quad 0 < t < 2/y^2, \quad (3.6)$$

and

$$\text{cdf}_{u_y(t, \cdot)}(x) = \begin{cases} 0, & -1 \leq x < 0 \\ \frac{x^2}{2t}, & 0 \leq x \leq \sqrt{2t}, \\ 1, & x > \sqrt{2t} \end{cases} \quad \forall t \geq 2/y^2. \quad (3.7)$$

The generalized inverse $\text{icdf}_{u_y(t, \cdot)} : [0, 1] \rightarrow \Omega$ has also an explicit expression which reads as

$$\text{icdf}_{u_y(t, \cdot)}(s) = \begin{cases} -1 & s = 0 \\ \sqrt{2ts}, & 0 < s < \frac{y^2 t}{2} \\ \frac{1}{y} \left(s + \frac{y^2 t}{2} \right), & \frac{y^2 t}{2} \leq s \leq 1, \end{cases} \quad 0 < t < 2/y^2 \quad (3.8)$$

and

$$\text{icdf}_{u_y(t, \cdot)}(s) = \begin{cases} -1 & s = 0 \\ \sqrt{2ts}, & 0 \leq s \leq 1, \end{cases} \quad \forall t \geq 2/y^2. \quad (3.9)$$

We can easily check that the set of solutions

$$\mathcal{M} = \{u(z) = u_y(t, \cdot) : z = (y, t) \in Z = [0, T] \times Y\}$$

is a subset of $\mathcal{P}_2(\Omega)$. As before, we introduce the set $\mathcal{T} := \{\text{Log}_w(u) : u \in \mathcal{M}\}$, where $w \in \mathcal{P}_2(\Omega)$, and prove the following result.

Lemma 3.3. *There exists a constant $C > 0$ such that for all $n \in \mathbb{N}^*$,*

$$d_n(\mathcal{T}, L^2(0, 1)) \leq Cn^{-11/6}. \quad (3.10)$$

Proof. Let us define

$$\tilde{\mathcal{T}} := \{\text{icdf}_u : u \in \mathcal{M}\} = \{\text{icdf}_{u(z)} : z \in Z\}.$$

It then obviously holds that

$$d_n(\mathcal{T}, L^2(0, 1)) \leq d_{n+1}(\tilde{\mathcal{T}}, L^2(0, 1)).$$

Thus, to prove (3.10), it is enough to prove that there exists $C > 0$ such that for all $n \in \mathbb{N}^*$,

$$d_n(\tilde{\mathcal{T}}, L^2(0, 1)) \leq Cn^{-11/6}. \quad (3.11)$$

Let us prove (3.11). To this aim, we prove two different auxiliary inequalities. Let $s_0 \in [0, 1]$ and $\varepsilon > 0$ so that $I_0 := [s_0 - \varepsilon/2, s_0 + \varepsilon/2] \subset [0, 1]$. We also denote by $W(I_0)$ the vectorial subspace of affine functions defined on I_0 . Now, let us consider $z := (y, t) \in Z$ such that $\frac{y^2 t}{2} \in [s_0 - \varepsilon/2, s_0 + \varepsilon/2]$. We denote by $P_{W(I_0)}$ the orthogonal projection of $L^2(I_0)$ onto $W(I_0)$. The Lipschitz constant of $P_{W(I_0)}(\text{icdf}_{u(z)} |_{I_0}) - \text{icdf}_{u(z)}$ on the interval I_0 is bounded by $\frac{1}{\sqrt{y}}$ and since $y \in [1/2, 3]$, it gives a bound on this interval

$$\sup_{s \in I_0} |P_{W(I_0)}(\text{icdf}_{u(z)} |_{I_0})(s) - \text{icdf}_{u(z)}(s)|^2 \leq \frac{\varepsilon^2}{\sqrt{2}}. \quad (3.12)$$

This implies that

$$\|P_{W(I_0)}(\text{icdf}_{u(z)} |_{I_0}) - \text{icdf}_{u(z)}\|_{L^2(I_0)} \leq \frac{\varepsilon^{3/2}}{\sqrt{2}}. \quad (3.13)$$

To go further, we make use of the following standard inequality: for all maps $f : [0, 1] \rightarrow \mathbb{R}$ whose differential is M -Lipschitz and all $s, s' \in [0, 1]$,

$$|f(s') - f(s) - f'(s)(s' - s)| \leq \frac{M}{2} |s - s'|^2. \quad (3.14)$$

For all $z := (y, t) \in Z$ such that $t > 0$ and $\frac{y^2 t}{2} \in I_0$, we consider the approximation of $\text{icdf}_{u(z)}$ using the function $g_{I_0} : I_0 \ni s \mapsto \sqrt{2ts}$, define the space $Z(I_0) := \text{Span}\{g_{I_0}\}$ and denote by $P_{Z(I_0)}$ the orthogonal projection of $L^2(I_0)$ onto $Z(I_0)$. We can apply the inequality (3.14) as follows. Since the Lipschitz constant of the first derivative of $\text{icdf}_{u(z)}$ is bounded by $|\frac{1}{2yt^3}|$ on the interval $[\frac{y^2 t}{2}, s_0 + \varepsilon/2]$. Therefore, we get the bound

$$\|\text{icdf}_{u(z)} - P_{Z(I_0)}(\text{icdf}_{u(z)}|_{I_0})\|_{L^2(I_0)} \leq \left| \frac{1}{4yt^3} \right| \varepsilon^{5/2}. \quad (3.15)$$

We are now in position to prove (3.11). Let $\beta > 1$ be a constant whose value will be fixed later on. Let $n \in \mathbb{N}^*$ and let us define for $1 \leq k \leq n$,

$$x_k := \frac{1}{2n^\beta} + (k-1)\frac{1}{n^\beta} \quad \text{and} \quad I_k := \left[x_k - \frac{1}{2n^\beta}, x_k + \frac{1}{2n^\beta} \right).$$

Besides, for all $n+1 \leq k \leq 2n$, we define

$$x_k := \frac{n}{n^\beta} + \frac{1}{2n} + (k-n-1)\frac{1}{n} \quad \text{and} \quad I_k := \left[\min\left(1, x_k - \frac{1}{2n}\right), \min\left(1, x_k + \frac{1}{2n}\right) \right).$$

In other words, the intervals $(I_k)_{1 \leq k \leq 2n}$ form a partition of the interval $[0, 1]$ so that the n first intervals (closest to the point $s = 0$) are of length $\frac{1}{n^\beta}$ and the other n intervals are of length at most $\frac{1}{n}$. We then define the space $V_n \subset L^2(0, 1)$ as follows:

$$V_n := \text{Span} \{ \mathbb{1}_{I_k}(s), \mathbb{1}_{I_k}(s)s, \mathbb{1}_{I_k}(s)\sqrt{s}, 1 \leq k \leq 2n \}.$$

In other words, V_n is composed of the functions which, on each interval I_k , is a linear combination of an affine function and the square root function. The dimension of the space V_n is at most $6n$. We denote by P_{V_n} the orthogonal projection of $L^2(0, 1)$ onto V_n .

It is easy to check that for all $z := (y, t) \in Z$,

$$\|P_{V_n}(\text{icdf}_{u(z)}) - \text{icdf}_{u(z)}\|_{L^2(0,1)} = \left\| P_{W(I_{k_0}) \oplus Z(I_{k_0})}(\text{icdf}_{u(z)}|_{I_{k_0}}) - \text{icdf}_{u(z)} \right\|_{L^2(I_{k_0})}$$

where I_{k_0} is the unique interval of $[0, 1]$ such that $\frac{y^2 t}{2} \in I_{k_0}$. On the one hand, if $1 \leq k_0 \leq n$, we make use of inequality (3.13) to obtain that

$$\left\| P_{W(I_{k_0}) \oplus Z(I_{k_0})}(\text{icdf}_{u(z)}|_{I_{k_0}}) - \text{icdf}_{u(z)} \right\|_{L^2(I_{k_0})} \leq \left\| P_{W(I_{k_0})}(\text{icdf}_{u(z)}|_{I_{k_0}}) - \text{icdf}_{u(z)} \right\|_{L^2(I_{k_0})} \leq \frac{n^{-3\beta/2}}{\sqrt{2}}.$$

On the other hand, if $n+1 \leq k_0 \leq 2n$, necessarily $\frac{y^2 t}{2} \geq \frac{n}{n^\beta}$, so that $4yt^3 \geq 2y^{-5}n^{3-3\beta}$. We then make use of inequality (3.15) to obtain that

$$\left\| P_{W(I_{k_0}) \oplus Z(I_{k_0})}(\text{icdf}_{u(z)}|_{I_{k_0}}) - \text{icdf}_{u(z)} \right\|_{L^2(I_{k_0})} \leq \left\| P_{Z(I_{k_0})}(\text{icdf}_{u(z)}|_{I_{k_0}}) - \text{icdf}_{u(z)} \right\|_{L^2(I_{k_0})} \leq \frac{4^5}{2} n^{-5/2-3+3\beta}.$$

Choosing now β such that $-3\beta/2 = -5/2 - 3 + 3\beta$, i.e. $\beta = 11/9$, we obtain that there exists a constant $C > 0$ such that for all $n \in \mathbb{N}^*$ and $z \in Z$,

$$\|P_{V_n}(\text{icdf}_{u(z)}) - \text{icdf}_{u(z)}\|_{L^2(0,1)} \leq Cn^{-11/6}.$$

This implies (3.11) and hence the desired result. \square

4 Algorithms for nonlinear reduced modelling in metric spaces

In this section, we introduce two methods for building in practice nonlinear reduced models for a set of solutions \mathcal{M} on general metric spaces. The methods involve a discrete training set $Z_{\text{tr}} \subset Z$ of $N \in \mathbb{N}^*$ parameters and associated N snapshot solutions $\mathcal{M}_{\text{tr}} \subset \mathcal{M}$. Similarly as before, we denote

$$\mathcal{T}_{\text{tr}} := \text{Log}_w(\mathcal{M}_{\text{tr}}) \subset \mathcal{T}$$

the image of \mathcal{M}_{tr} by the logarithmic map Log_w , where w is an element of $\mathcal{P}_2(\Omega)$ to be fixed in a moment. Since our numerical tests are for one-dimensional conservative PDEs in W_2 , we also instantiate them in this setting.

4.1 Tangent PCA (tPCA): offline stage

Our first method is based on the so-called Tangent PCA (tPCA) method. Its definition requires that the metric space (V, d) is embedded with a Riemannian structure. The tPCA method consists in mapping the manifold to a tangent space and performing a standard PCA on this linearization.

In the offline phase of the tPCA method, we first fix a particular element $w \in \mathcal{M}$, usually the Fréchet mean

$$\min_{\tilde{w} \in V} \frac{1}{N} \sum_{u \in \mathcal{M}_{\text{tr}}} d(u, \tilde{w})^2,$$

and then define an inner product g_w on its tangent space $T_w V$. We next consider the PCA (or POD decomposition) on $T_w V$ of the set

$$\mathcal{T}_{\text{tr}} := \text{Log}_w(\mathcal{M}_{\text{tr}}),$$

with respect to the inner product g_w . For every $f \in T_w V$, its norm is denoted by $\|f\|_w = g_w^{1/2}(f, f)$. There exists an orthonormal family of functions $(f_k)_{k \geq 1}^N$ of $T_w V$ and an orthogonal family $(c_k)_{k \geq 1}$ of functions of $\ell^2(\mathcal{Z}_{\text{tr}})$ norm such that

$$\text{Log}_w(u(z)) = \sum_{k=1}^N c_k(z) f_k, \quad \forall z \in \mathcal{Z}_{\text{tr}}.$$

The k^{th} singular value is defined as $\sigma_k := \|c_k\|_{\ell^2(\mathcal{Z}_{\text{tr}})}$ and we arrange the indices so that $(\sigma_k)_{k \geq 1}$ is a non-increasing sequence.

In the online phase, we fix $n \in \mathbb{N}^*$ and define $V_n := \text{Span}(f_1, \dots, f_n)$ and P_{V_n} the orthogonal projection on $T_w V$ with respect to the scalar product g_w . For a given $z \in \mathcal{Z}$ for which we want to approximate $u(z)$, we consider two possible versions:

- **Projection:** We compute

$$f_n^{\text{proj}}(z) := P_{V_n} \text{Log}_w(u(z)) = \sum_{k=1}^n c_k(z) f_k, \quad (4.1)$$

and approximate $u(z)$ as

$$u_n(z)^{\text{tPCA,proj}} := \text{Exp}_w(f_n^{\text{proj}}(z)). \quad (4.2)$$

Note that, in fact, the projection (4.1) cannot be computed online since the computation of the coefficients $c_k(z)$ requires the knowledge of $\text{Log}_w(u(z))$ (and thus of the snapshot $u(z)$ itself). This motivates the following strategy based on interpolation of the $c_k(z)$.

- **Interpolation:** Among the possible ways to make the method applicable online, we propose to compute an interpolation $\bar{c}_k : \mathcal{Z} \rightarrow \mathbb{R}$ such that

$$\bar{c}_k(z) = c_k(z), \quad \forall z \in \mathcal{Z}_{\text{tr}}, 1 \leq k \leq n.$$

In the numerical experiments, to avoid stability problems, we restrict the interpolation to neighboring parameters of the target parameter z which belong to the training set \mathcal{Z}_{tr} . Specifically, for a given fixed tolerance $\tau > 0$, we find the set $\mathcal{N}_\tau(z, \mathcal{Z}_{\text{tr}})$ of parameters of \mathcal{Z}_{tr} whose ℓ^2 -distance to the current z is at most τ , that is,

$$\mathcal{N}_\tau(z, \mathcal{Z}_{\text{tr}}) := \{\tilde{z} \in \mathcal{Z}_{\text{tr}} : \|z - \tilde{z}\|_{\ell^2(\mathbb{R}^p)} \leq \tau\}.$$

Then, for $k = 1, \dots, n$, we build a local spline interpolator $\bar{c}_k^{z, \tau}$ that satisfies the local interpolating conditions

$$\bar{c}_k^{z, \tau}(z) = c_k(z), \quad \forall z \in \mathcal{N}_\tau(z, \mathcal{Z}_{\text{tr}}).$$

With the local interpolators $\bar{c}_k^{z, \tau}$, we now compute

$$f_n^{\text{interp}}(z) := \sum_{k=1}^n \bar{c}_k^{z, \tau}(z) f_k. \quad (4.3)$$

which is an online computable approximation of $\text{Log}_w(u(z))$. Finally, we approximate $u(z)$ with

$$u_n(z)^{\text{tPCA,interp}} := \text{Exp}_w(f_n^{\text{interp}}(z)). \quad (4.4)$$

Before continuing, several comments are in order:

- In the online phase, it is necessary to compute exponential maps. However, in full generality, their computation may be expensive since it may require to solve a problem in the full space and not only in a reduced space. This important issue is mitigated in our numerical examples because the exponential map in W_2 in one space dimension has an explicit expression. The development of efficient surrogates for the exponential mapping is a topic by itself which we will address in future works.
- Note that $u_n^{\text{tPCA,proj}}(z)$ or $u_n^{\text{tPCA,interp}}(z)$ are not always properly defined through (4.2) or (4.4) since it is required that $f_n^{\text{proj}}(z)$ or $f_n^{\text{interp}}(z)$ belong to \mathcal{O}_w , the definition domain of the map Log_w . Since there is a priori no guarantee that this is always the case, the approach does not lead to a fully robust numerical method and is prone to numerical instabilities as we illustrate in our numerical examples. This drawback has been one main motivation to develop the method based on barycenters, which will be stable by construction. We emphasize nonetheless that the tPCA has important optimality properties in terms of its decay of the approximation error as we describe next. This is probably the reason why numerical methods based on tPCA have drawn significant interest in numerous fields like pattern recognition, shape analysis, medical imaging, computer vision [26, 56], and, more recently, statistics [35] and machine learning to study families of histograms and probability densities [18]. We show evidence that this method also carries potential for model reduction of transport dominated systems in Section 6.

Error decay: By introducing a notion of resolution of the finite set \mathcal{T}_{tr} with respect to \mathcal{T} in terms of ε -coverings, we can derive a convergence result on the average error in \mathcal{T} which is, as defined in (1.5),

$$e_{\text{av}}^{\text{tPCA,proj}}(\mathcal{T}, T_w V, V_n) = \left(\int_{z \in \mathcal{Z}} \|\text{Log}_w u(z) - P_{V_n} \text{Log}_w(u(z))\|_w^2 d\mu(z) \right)^{1/2}$$

We next recall the precise definition of ε -covering of a set and its covering number and give a convergence result of the error.

Definition 4.1 (ε -covering and covering number). Let S be a subset of a metric space (V, d) . An ε -covering of S is a subset C of S if and only if $S \subseteq_{x \in C} B(x, \varepsilon)$, where $B(x, \varepsilon)$ denotes the ball centered at x of radius ε . The covering number of S , denoted $N_S(\varepsilon)$, is the minimum cardinality of any ε -covering of S .

Lemma 4.2. *If \mathcal{T}_{tr} is an ε -covering of \mathcal{T} , then*

$$\delta_n(\mathcal{T}, T_w V) \leq e_{\text{av}}^{\text{tPCA,proj}}(\mathcal{T}, T_w V, V_n) \leq \varepsilon + \left(\sum_{k > n}^M \sigma_k^2 \right)^{1/2}, \quad (4.5)$$

where $\delta_n(\mathcal{T}, T_w V)$ is the L^2 -Kolmogorov n -width of \mathcal{T} in the space $(T_w V, \|\cdot\|_w)$ as defined in (1.7). In addition, if the exponential mapping Exp_w satisfies Hypothesis 3.1 and if

$$f_n^{\text{proj}}(z) = P_{V_n} \text{Log}_w(u(z)) \in \mathcal{O}_w, \quad \forall z \in \mathcal{Z},$$

then

$$e_{\text{av}}^{\text{tPCA,proj}}(\mathcal{M}, V, V_n) := \left(\int_{z \in \mathcal{Z}} d(u(z), u_n(z))^{\text{tPCA,proj}} d\mu(z) \right)^{1/2} \leq \underline{c}^{-1} \varepsilon + \underline{c}^{-1} \left(\sum_{k > n}^M \sigma_k^2 \right)^{1/2}.$$

Proof. The lower bound of (4.5) simply follows by the definition of $\delta_n(\mathcal{T}, T_w V)$. As for the upper bound, since for any $u \in \mathcal{T}$, there exists $\tilde{u} \in \mathcal{T}_{\text{tr}}$ such that $\|u - \tilde{u}\|_w \leq \varepsilon$, then $\|u - P_{V_n} u\|_w \leq \varepsilon + \|\tilde{u} - P_{V_n} \tilde{u}\|_w$. Thus

$$\underline{c} e_{\text{av}}^{\text{tPCA,proj}}(\mathcal{M}, V, V_n) \leq e_{\text{av}}^{\text{tPCA,proj}}(\mathcal{T}, T_w V, V_n) \leq \varepsilon + e_{\text{av}}^{\text{tPCA,proj}}(\mathcal{T}_{\text{tr}}, T_w V, V_n) = \varepsilon + \left(\sum_{k > n}^N \sigma_k^2 \right)^{1/2}.$$

□

In the particular case of the Wasserstein space $(V, d) = (\mathcal{P}_2(\Omega), W_2)$, the offline phase of the tPCA method consists in performing the following steps:

- Compute $\bar{f} := \frac{1}{N} \sum_{u \in \mathcal{M}_{\text{tr}}} \text{icdf}_u$ and $w = \text{icdf}^{-1}(\bar{f})$.
- Compute

$$\mathcal{T}_{\text{tr}} := \{\text{icdf}_u - \text{icdf}_w : u \in \mathcal{M}_{\text{tr}}\} \subset L^2([0, 1]).$$

- Compute the n first modes of the PCA of the discrete set of functions \mathcal{T}_{tr} in $L^2([0, 1])$ and denote them by f_1, \dots, f_n ;
- Similarly as before, there exists an orthonormal family of functions $(f_k)_{k \geq 1}^N$ of $L^2([0, 1])$ and an orthogonal family $(c_k)_{k \geq 1}$ of functions of $\ell^2(\mathbb{Z}_{\text{tr}})$ with non-increasing ℓ^2 norm such that for all $z \in \mathbb{Z}_{\text{tr}}$,

$$\text{Log}_w(u(z)) = \sum_{k=1}^N c_k(z) f_k, \quad \forall z \in \mathbb{Z}_{\text{tr}}.$$

The k^{th} singular value is defined as $\sigma_k := \|c_k\|_{\ell^2(\mathbb{Z}_{\text{tr}})}$ and

$$c_k(z) := \langle \text{icdf}_{u(z)} - \text{icdf}_w, f_k \rangle_{L^2(0,1)}.$$

For the online phase, if we work with a dimension $n \in \mathbb{N}^*$ for the reduced space, we store the coefficients $c_k(z)$ for all $z \in \mathbb{Z}_{\text{tr}}$ and $1 \leq k \leq n$.

In the online stage, we fix a dimension $n \in \mathbb{N}^*$ and, for a given target $z \in \mathbb{Z}$ for which we want to approximate $u(z)$, we perform the following steps:

- **Projection:** Compute for all $1 \leq k \leq n$,

$$c_k(z) := \langle \text{icdf}_{u(z)} - \text{icdf}_w, f_k \rangle_{L^2([0,1])}$$

and

$$f_n^{\text{proj}}(z) := \sum_{k=1}^n c_k(z) f_k.$$

The reduced-order model approximation $u_n(z)^{\text{tPCA,proj}}$ of $u(z)$ then reads as

$$u_n(z)^{\text{tPCA,proj}} := \text{icdf}^{-1} \left(\text{icdf}_w + f_n^{\text{proj}}(z) \right), \quad (4.6)$$

provided that $f_n^{\text{proj}}(z)$ belongs to $\mathcal{K}_{\text{icdf}_w}$.

- **Interpolation:** For all $1 \leq k \leq n$, from the knowledge of the values $(c_k(z))_{z \in \mathbb{Z}_{\text{tr}}}$ stored in the offline phase, we compute an interpolation $\bar{c}_k : \mathbb{Z} \rightarrow \mathbb{R}$ such that

$$\bar{c}_k(z) = c_k(z), \quad \forall z \in \mathbb{Z}_{\text{tr}}, 1 \leq k \leq n.$$

We can proceed similarly as before and do a local interpolation. We then compute

$$f_n^{\text{interp}}(z) := \sum_{k=1}^n \bar{c}_k(z) f_k, \quad (4.7)$$

and approximate $u(z)$ with

$$u_n(z)^{\text{tPCA,interp}} := \text{icdf}^{-1} \left(\text{icdf}_w + f_n^{\text{interp}}(z) \right), \quad (4.8)$$

provided that $f_n^{\text{interp}}(z)$ belongs to $\mathcal{K}_{\text{icdf}_w}$.

Error decay: As a direct consequence of Lemma 4.2 and Corollary 2.3, we have the following result on the average approximation error in \mathcal{M} ,

$$e_{\text{av}}^{\text{tPCA,proj}}(\mathcal{M}, W_2, V_n) := \int_{z \in \mathbb{Z}} W_2 \left(u(z), u_n(z)^{\text{tPCA,proj}} \right) d\mu(z).$$

Corollary 4.3. *If \mathcal{T}_{tr} is an ε -covering of \mathcal{T} , and if $f_n^{\text{proj}}(z) \in \mathcal{K}_{\text{icdf}_w}$ for all $z \in \mathbb{Z}$, then*

$$e_{\text{av}}^{\text{tPCA,proj}}(\mathcal{M}, W_2, V_n) \leq \varepsilon + \left(\sum_{k > n}^M \sigma_k^2 \right)^{1/2}.$$

4.2 The barycentric greedy algorithm (gBar)

The potential instabilities of the tPCA method lead us to consider an alternative strategy for the construction of reduced-order models, based on the use of barycenters [53]. The approach that we propose here can be defined for general metric spaces (V, d) which may not be embedded with a Riemannian manifold structure. Contrary to tPCA, it is guaranteed to be stable in the sense that all the steps of the algorithm are well-defined (approximations in $T_w V$ will be in \mathcal{O}_w by construction). The stability comes at the price of difficulties in connecting theoretically its approximation quality with optimal performance quantities. Thus its quality will be evaluated through numerical examples.

The method relies on a greedy algorithm, and is henceforth referred to hereafter as the *barycentric greedy* (gBar) method. Let $\varepsilon > 0$ be a prescribed level of accuracy. The offline phase of the gBar method is an iterative algorithm which can be written as follows:

- **Initialization:** Compute $(z_1, z_2) \in Z_{\text{tr}} \times Z_{\text{tr}}$ such that

$$(z_1, z_2) \in \underset{(\tilde{z}_1, \tilde{z}_2) \in Z_{\text{tr}} \times Z_{\text{tr}}}{\operatorname{argmax}} d(u(\tilde{z}_1), u(\tilde{z}_2))^2,$$

and define $U_2 := \{u(z_1), u(z_2)\}$. Then compute

$$\Lambda_2(z) \in \underset{\Lambda_2 \in \Sigma_2}{\operatorname{argmin}} d(u(z), \operatorname{Bar}(U_2, \Lambda_2))^2, \quad \forall z \in Z_{\text{tr}}.$$

- **Iteration $n \geq 3$:** Compute $z_n \in Z_{\text{tr}}$ such that

$$z_n \in \underset{\tilde{z} \in Z_{\text{tr}}}{\operatorname{argmax}} \min_{b \in \mathcal{B}_{n-1}(U_{n-1})} d(u(\tilde{z}), b)^2.$$

and set $U_n := U_{n-1} \cup \{u(z_n)\}$. Then compute

$$\Lambda_n(z) \in \underset{\Lambda_n \in \Sigma_n}{\operatorname{argmin}} d(u(z), \operatorname{Bar}(U_n, \Lambda_n))^2, \quad \forall z \in Z_{\text{tr}}.$$

The algorithm terminates when

$$\max_{\tilde{z} \in Z_{\text{tr}}} \min_{b \in \mathcal{B}_{n-1}(U_{n-1})} d(u(\tilde{z}), b)^2 = \min_{b \in \mathcal{B}_{n-1}(U_{n-1})} d(u(z_n), b)^2 < \varepsilon^2.$$

Note that the gBar algorithm selects via a greedy procedure particular snapshots $U_n = \{u(z_1), \dots, u(z_n)\}$ in order to approximate as well as possible each element $u(z) \in \mathcal{M}_{\text{tr}}$ with its optimal barycenter associated to the family U_n . The barycentric weights have to be determined via an optimization procedure.

Similarly to the tPCA method, we can consider two different versions of the online phase of the gBar algorithm, whose aim is to reconstruct, for a given $n \in \mathbb{N}^*$, a reduced-model approximation $u_n^{\text{gBar}}(z)$ of $u(z)$ for all $z \in Z$. These two different versions consist in the following steps:

- **Projection:** Let $z \in Z$. Compute $\Lambda_n(z) \in \Sigma_n$ a minimizer of

$$\Lambda_n(z) \in \underset{\Lambda_n \in \Sigma_n}{\operatorname{argmin}} d(u(z), \operatorname{Bar}(U_n, \Lambda_n))^2,$$

and choose $u_n^{\text{gBar,proj}}(z) \in \operatorname{Bar}(U_n, \Lambda_n(z))$.

- **Interpolation:** From the values $(\Lambda_n(z))_{z \in Z_{\text{tr}}}$ which are known from the offline stage, compute an interpolant $\bar{\Lambda}_n : Z \rightarrow \Sigma_n$ such that

$$\bar{\Lambda}_n(z) = \Lambda_n(z), \quad \forall z \in Z_{\text{tr}}.$$

For a given $z \in Z$, we approximate $u(z)$ with $u_n^{\text{gBar,interp}}(z) \in \operatorname{Bar}(U_n, \bar{\Lambda}_n(z))$.

As for the tPCA method, the only efficient online strategy is the one based on the interpolation of the barycentric coefficients, since the projection method requires the computation of the full solution $u(z)$ for $z \in Z$. We consider both strategies to compare their quality of approximation in our numerical tests.

In the particular case when $(V, d) = (\mathcal{P}_2(\Omega), W_2)$, every step of the greedy barycentric algorithm can be made explicit by means of inverse cumulative distribution functions. The offline phase is:

- **Initialization:** Compute $(z_1, z_2) \in Z_{\text{tr}} \times Z_{\text{tr}}$ such that

$$(z_1, z_2) \in \underset{(\tilde{z}_1, \tilde{z}_2) \in Z_{\text{tr}} \times Z_{\text{tr}}}{\operatorname{argmax}} \left\| \operatorname{icdf}_{u(\tilde{z}_1)} - \operatorname{icdf}_{u(\tilde{z}_2)} \right\|_{L^2(0,1)}^2,$$

and define $U_2 := (u(z_1), u(z_2))$. Compute and store

$$\Lambda_2(z) := (\lambda_1^2(z), \lambda_2^2(z)) \in \underset{\Lambda_2 := (\lambda_1, \lambda_2) \in \Sigma_2}{\operatorname{argmin}} \left\| \operatorname{icdf}_{u(z)} - \sum_{k=1}^2 \lambda_k \operatorname{icdf}_{u(z_k)} \right\|_{L^2(0,1)}^2, \quad \forall z \in Z_{\text{tr}}. \quad (4.9)$$

- **Iteration $n \geq 3$:** Given the set of barycentric coefficients

$$\Lambda_{n-1}(z) := (\lambda_1^{n-1}(z), \dots, \lambda_{n-1}^{n-1}(z)), \quad \forall z \in Z_{\text{tr}}.$$

from the previous iteration, find

$$\begin{aligned} z_n &\in \underset{z \in Z_{\text{tr}}}{\operatorname{argmax}} \min_{\Lambda_{n-1} := (\lambda_1, \dots, \lambda_{n-1}) \in \Sigma_{n-1}} \left\| \operatorname{icdf}_{u(z)} - \sum_{k=1}^{n-1} \lambda_k \operatorname{icdf}_{u(z_k)} \right\|_{L^2(0,1)}^2 \\ &= \underset{z \in Z_{\text{tr}}}{\operatorname{argmax}} \left\| \operatorname{icdf}_{u(z)} - \sum_{k=1}^{n-1} \lambda_k^{n-1}(z) \operatorname{icdf}_{u(z_k)} \right\|_{L^2(0,1)}^2 \end{aligned}$$

and set $U_n := U_{n-1} \cup \{u(z_n)\}$. Compute and store

$$\Lambda_n(z) := (\lambda_1^n(z), \dots, \lambda_n^n(z)) \in \underset{\Lambda_n := (\lambda_1, \dots, \lambda_n) \in \Sigma_n}{\operatorname{argmin}} \left\| \operatorname{icdf}_{u(z)} - \sum_{k=1}^n \lambda_k \operatorname{icdf}_{u(z_k)} \right\|_{L^2(0,1)}^2, \quad \forall z \in Z_{\text{tr}}. \quad (4.10)$$

The algorithm terminates if

$$\min_{\Lambda_{n-1} := (\lambda_1, \dots, \lambda_{n-1}) \in \Sigma_{n-1}} \left\| \operatorname{icdf}_{u(z_n)} - \sum_{k=1}^{n-1} \lambda_k \operatorname{icdf}_{u(z_k)} \right\|_{L^2(0,1)}^2 < \varepsilon^2.$$

For a fixed $n \in \mathbb{N}^*$, the two versions of the online phase of the gBar method read as follows:

- **Projection:** Given $z \in Z$ for which we want to approximate $u(z)$, compute

$$\Lambda_n(z) \in \underset{\Lambda_n := (\lambda_1, \dots, \lambda_n) \in \Sigma_n}{\operatorname{argmin}} \left\| \operatorname{icdf}_{u(z)} - \sum_{k=1}^n \lambda_k \operatorname{icdf}_{u(z_k)} \right\|_{L^2(0,1)}^2, \quad (4.11)$$

and define $u_n^{\text{gBar,proj}}(z) = \operatorname{Bar}(U_n, \Lambda_n(z))$. The function $u_n^{\text{gBar,proj}}(z) \in \mathcal{P}_2(\Omega)$ can easily be defined through its icdf as

$$\operatorname{icdf}_{u_n^{\text{gBar,proj}}(z)} = \sum_{k=1}^n \lambda_k(z) \operatorname{icdf}_{u(z_k)}.$$

- **Interpolation:** From the known values $(\Lambda_n(z))_{z \in Z_{\text{tr}}}$, compute an interpolation $\bar{\Lambda}_n : Z \rightarrow \Sigma_n$ such that

$$\bar{\Lambda}_n(z) = \Lambda_n(z), \quad \forall z \in Z_{\text{tr}}.$$

For a given target $u(z)$ with $z \in Z$, we approximate with $u_n^{\text{gBar,interp}}(z) = \operatorname{Bar}(U_n, \bar{\Lambda}_n(z))$ which is the function of $\mathcal{P}_2(\Omega)$ such that

$$\operatorname{icdf}_{u_n^{\text{gBar,interp}}(z)} = \sum_{k=1}^n \bar{\lambda}_k(z) \operatorname{icdf}_{u(z_k)},$$

where $\bar{\Lambda}_n(z) = (\bar{\lambda}_1(z), \dots, \bar{\lambda}_n(z))$.

Notice that (4.9) and (4.10) amounts to solving a simple quadratic programming problem on a convex cone.

5 Numerical cost

We give simple estimates on the numerical complexity of the tPCA and gBar methods in terms of the number of operations. We consider the versions where we do interpolation instead of projection. For this, we introduce some preliminary notation. Let $\text{cost}(u(z))$ be the numerical cost to compute a given snapshot $u(z) = u(t, y)$. If the full-order PDE discretization has a uniform spatial mesh with \mathcal{N} degrees of freedom and uses a simple implicit Euler time integration with time step δt , then $\text{cost}(u(z)) \sim \mathcal{N}^3 t / \delta t$ with a direct linear system solver, or $\text{cost}(u(z)) \sim k \mathcal{N}^2 t / \delta t$ with an iterative solver requiring k iterations to converge. Let $\text{cost}(\text{Log}_w)$ and $\text{cost}(\text{Exp}_w)$ be the cost of computing the logarithmic and exponential maps.

tPCA: In the offline phase, we have to compute N snapshots, compute their logarithmic images to get \mathcal{T}_{tr} , and perform a PCA on \mathcal{T}_{tr} . Thus $\text{cost}_{\text{offline}}^{\text{tPCA}} = \sum_{z \in \mathcal{Z}_{\text{tr}}} \text{cost}(u(z)) + N \text{cost}(\text{Log}_w) + \text{cost}^{\text{PCA}}$. Counting the cost of computing the covariance matrix and the eigenvalue computation, we have $\text{cost}^{\text{PCA}} \sim N \mathcal{N}^2 + \mathcal{N}^3$. Therefore

$$\text{cost}_{\text{offline}}^{\text{tPCA}} \sim N(\mathcal{N}^3 T / \delta t + \text{cost}(\text{Log}_w)) + N \mathcal{N}^2 + \mathcal{N}^3.$$

For a given $z \in \mathcal{Z}$, to approximate $u(z)$ with $u_n(z)^{\text{tPCA,interp}}$ in the online phase, we have to compute an interpolant and an exponential mapping. If we do the local interpolation of each coefficient $c_k(z)$ with r neighbors, the cost of the interpolation is of order $r^3 + p \ln(N)$, where r^3 is the cost to solve the final linear system and $p \ln(N)$ is the cost of finding the r nearest neighbors with state of the art algorithms like the ball tree. As a result

$$\text{cost}(u_n(z)^{\text{tPCA,interp}}) \sim n(r^3 + p \ln(N)) + \text{cost}(\text{Exp}_w),$$

This cost has to be compared to $\text{cost}(u(z)) \sim \mathcal{N}^3 t / \delta t$, the cost of computing $u(z)$ with the full order model. We clearly see the critical role that the cost of the exponential mapping plays in the efficiency of the reduction method. As already brought up in section 4.1, $\text{cost}(\text{Exp}_w)$ can in general be expensive since it may require to solve a problem in the full space. In the case of W_2 in one space dimension, the cost is strongly reduced since the exponential map has an explicit expression. The problem of building good surrogates of the exponential mapping is a topic by itself and its treatment is deferred to future works.

gBar: If we perform n steps in the barycentric greedy algorithm, the cost scales like

$$\text{cost}_{\text{offline}}^{\text{gBar}} \sim N(\mathcal{N}^3 T / \delta t + \text{cost}(\text{Log}_w) + n \text{cost}_n(\text{best Bar}))$$

where $\text{cost}_n(\text{best Bar})$ is the cost of computing the best barycenter of a function u with respect to a set U_n of n functions. It is equal to the complexity of solving the cone quadratic optimization problem (2.14) and is typically proportional to n^2 . In the online phase, the cost to approximate a given target $u(z)$ is

$$\text{cost}(u_n(z)^{\text{tPCA,interp}}) \sim r^3 + p \ln(N) + \text{cost}(\text{Exp}_w).$$

Like before, the cost $\text{cost}(\text{Exp}_w)$ is the critical part for the efficiency.

6 Numerical examples

As a support for our tests, we consider four different conservative PDEs:

- The above discussed inviscid Burger's equation for which we have explicit expressions of the solutions and icdf (see section 3.2).
- The version with viscosity of the previous Burger's equation.
- A Camassa Holm equation.
- A Korteweg de Vries equation.

For each PDE, we compare the performance of the four following model reduction methods:

- The classical PCA method in L^2 ,
- The tangent PCA method (with projection) in W_2 ,
- The gBar method (with interpolation and projection) in W_2 .

The performance is measured in terms of the average and worst case approximation error of a set on a discrete test set of 500 functions. Each test set is different from the training set \mathcal{M}_{tr} (also composed of 500 functions).

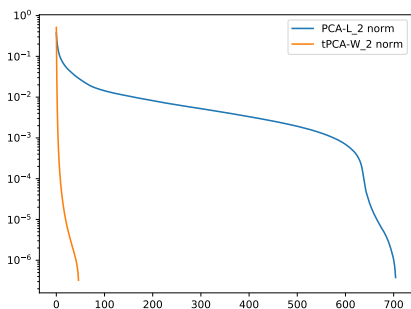
The code to reproduce the numerical results is available online at:

<https://github.com/olga-mula/2019-RBM-metric-spaces>

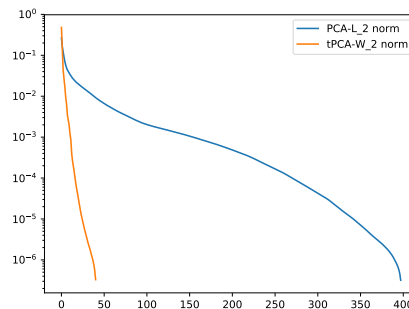
For each PDE example, we also provide reconstruction videos of a full propagation on the same link.

6.1 Inviscid Burger's equation

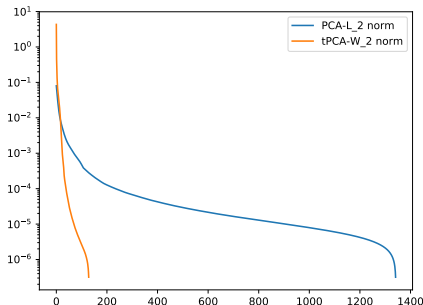
We consider the same parametric PDE as the one of section 3.2 and focus first on the average error decay of PCA and tPCA in the training set \mathcal{M}_{tr} , denoted by $e_{\text{av}}(\mathcal{M}_{\text{tr}}, L^2, V_n^{\text{PCA}})$ and $e_{\text{av}}(\mathcal{M}_{\text{tr}}, W_2, V_n^{\text{tPCA}})$. Figure 1a shows that the error with tPCA decreases much faster than the one with PCA. This is connected to the fact that the decay of the n -width $\delta_n(\mathcal{M}, L^2(\Omega))$ and associated singular values is much slower than $\delta_n(\mathcal{T}, L^2([0, 1]))$, which is the width exploited in tPCA (see sections 3.2 and 4.1).



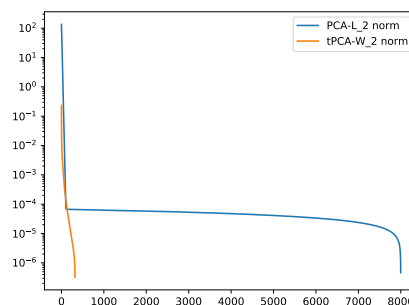
(a) Burgers equation.



(b) Viscous Burgers equation.



(c) CH equation.



(d) KdV equation.

Figure 1: Convergence of average errors in training set.

Figure 2 gives the errors in average and worst case over $\mathcal{M}_{\text{test}}$. The plots on the left measure the errors in the natural norm of each method, that is, L^2 for PCA and W_2 for the rest. Note first of all the dramatic difference in the behavior of the error between PCA (which is very slow) and the rest of the approaches (which is much faster). Also, we can see that tPCA presents a faster decay rate compared to the approach with barycenters. This may lead to think that tPCA is a better choice for the present context but to confirm this it is necessary to measure errors in a common metric which is “fair” for all approaches and which also quantifies the potential numerical instabilities of tPCA. Since we are looking for metrics that quantify the quality of transport rather than spatial averages, we discard the L^2 metric in favor of the H^{-1} metric which can be seen as a relaxation of W_2 . The plots on the right in Figure 2 measure the errors in this norm. We again observe the superiority of tPCA and the barycenters’ approach with respect to the PCA. The plateau that tPCA and the approach with barycenters reach at a value around 10^{-3} is due to the fact that the H^{-1} requires to invert a Laplace operator. For this, we used in our case a discretization with P1 finite elements on

a spatial mesh of size $h \approx 5.10^{-4}$. So the plateau is due to this discretization error and not to the fact that the approximation errors do not tend to 0.

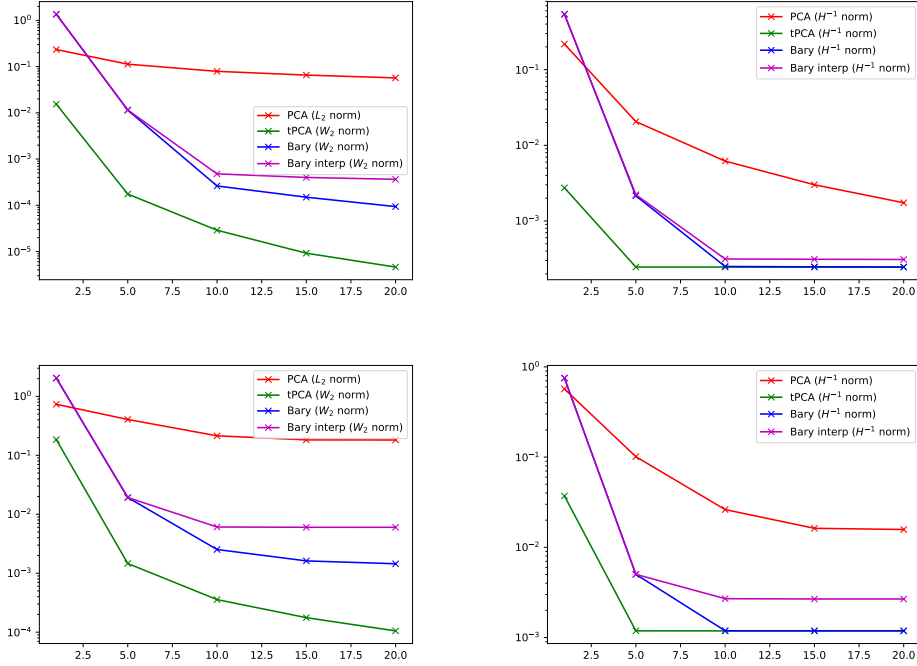


Figure 2: Errors on $\mathcal{M}_{\text{test}}$ for the Burgers equation. Top figures: average error. Bottom figures: worst case error. Left: natural norms. Right: H^{-1} norm.

In Figure 6 of Appendix A, we give plots of the reconstruction of one snapshot with all the methods. The PCA approach presents very strong oscillations and fails to capture the sharp-edged form of the snapshot. tPCA and the approach with barycenters give an approximation of higher quality in terms of the “shape” of the reconstructed function. The tPCA approximation presents unnatural “spikes” which are due to the instabilities described in section 4.1. We also provide videos of the reconstruction of a full evolution with our methods on the link above.

6.2 Viscous Burger’s equation

We consider the same problem as before but add a viscosity term ν that ranges in $[5.10^{-5}, 0.1]$. The equation is then

$$u_t + \frac{1}{2}(u^2)_x - \nu \partial_x^2 u = 0, \quad u(0, x, y) = \begin{cases} 0, & -3 \leq x < 0 \\ y, & 0 \leq x < \frac{1}{y} \\ 0, & \frac{1}{y} \leq x \leq 5, \end{cases} \quad (6.1)$$

where, like before, the parameter $y \in [1/2, 3]$ and $(t, x) \in [0, T] \times \Omega = [0, 3] \times [-3, 5]$ (the space interval has slightly been enlarged). The parameter domain is here

$$\mathcal{Z} = \{(t, y, \nu) \in [0, 3] \times [0.5, 3] \times [5.10^{-5}, 0.1]\}.$$

We present the results following the same lines as in the previous example. Figure 1b shows the decay of the error of the PCA and tPCA methods in the average sense and for the functions used in the training phase. Like before, the error decays dramatically faster in tPCA than in PCA.

Next, Figure 3 gives the errors in average and worst case sense for the test set $\mathcal{M}_{\text{test}}$. If we first examine the errors in the natural norms (plots on the left), it appears that the errors in tPCA do not seem to decay significantly faster than in PCA. Also, the approach with barycenters does not seem to give a very good performance and seems to perform worse than PCA. However, when we examine the errors in the unified H^{-1} metric, we see that all the nonlinear methods are clearly outperforming

PCA. This is more in accordance with what we visually observe when we examine the reconstructed functions given by each method (see Figure 7 of Appendix A). Like before, the approximation with PCA has unnatural oscillations. Note that in this particular example the tPCA presents a sharp unnatural spike at the propagation front, due to the above discussed stability issues of this method. This is in contrast to the approach with barycenters which does not suffer from this issue at the cost of slightly degrading the final approximation quality. Like for the other examples, the reader may watch videos of the reconstruction on the link above.

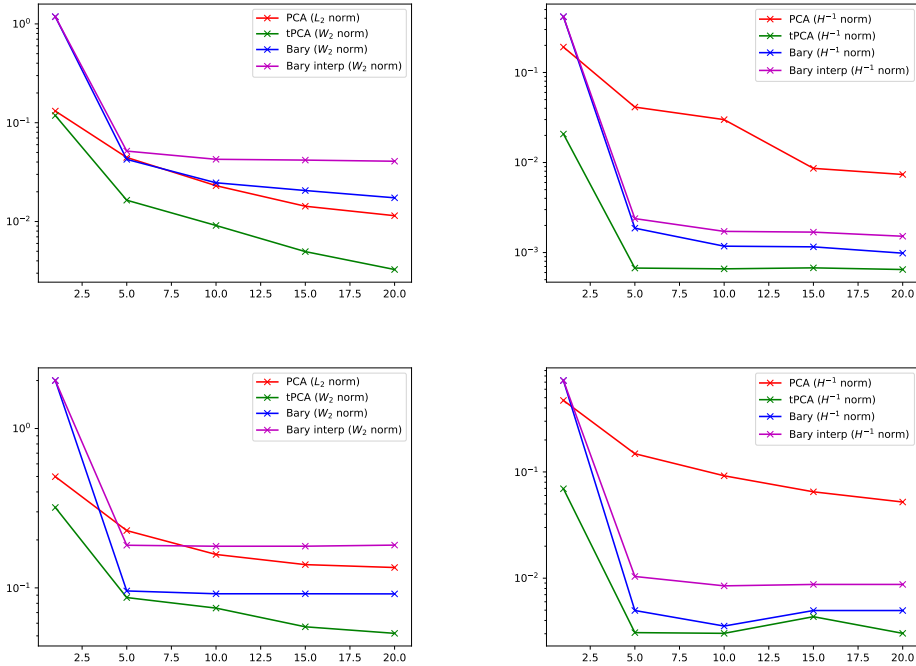


Figure 3: Errors on $\mathcal{M}_{\text{test}}$ for the Viscous Burgers equation. Top figures: average error. Bottom figures: worst case error. Left: natural norms. Right: H^{-1} norm.

6.3 The Camassa-Holm equation

We next consider the dispersionless Camassa-Holm equation which, for $\alpha > 0$ given, consists in finding the solution u of

$$\partial_t m + um_x + 2m\partial_x u = 0, \quad \text{with } m = u - \alpha^2 \partial_{xx} u. \quad (6.2)$$

The equation admits peakon solutions of the form

$$u(t, x) = \frac{1}{2} \sum_{i=1}^N p_i(t) e^{-|x - q_i(t)|/\alpha},$$

where the evolution of the set of peakon parameters $p_i(t)$ and $q_i(t)$ satisfies the canonical Hamiltonian dynamics

$$\dot{q}_i(t) = \frac{\partial h_N}{\partial p_i} \quad \text{and} \quad \dot{p}_i(t) = -\frac{\partial h_N}{\partial q_i} \quad (6.3)$$

for $i = 1, \dots, N$, with Hamiltonian given by

$$h_N = \frac{1}{4} \sum_{i,j=1}^N p_i p_j e^{-|q_i - q_j|/\alpha}. \quad (6.4)$$

For the parametrized model considered in our tests, we set $N = 2$ and $\alpha = 1$. The initial values of the peakons parameters are $p_1(0) = 0.2$, $p_2(0) = 0.8$, $q_1(0) \in [-2, 2]$ and $q_2(0) = -5$. The parameter domain is then

$$\mathcal{Z} = \{(t, q_1(0)) \in [0, 40] \times [-2, 2]\}.$$

Figure 1c shows the decay of the error of the PCA and tPCA methods in the average sense and for the functions used in the training phase. Like before, the error decays dramatically faster in tPCA than in PCA.

Figure 4 gives the errors in average and worst case sense for the test set $\mathcal{M}_{\text{test}}$. Very similar observations like for the case of Viscous Burger's hold: in the natural norms, the errors in tPCA do not seem to decay significantly faster than in PCA. The approach with barycenters does not seem to give a very good performance and seems to perform worse than PCA. Very different conclusions can be drawn if we consider the unified H^{-1} metric, where we see that all the nonlinear methods are clearly outperforming PCA. Like previously, this is confirmed visually (see Figure 8 of Appendix A).

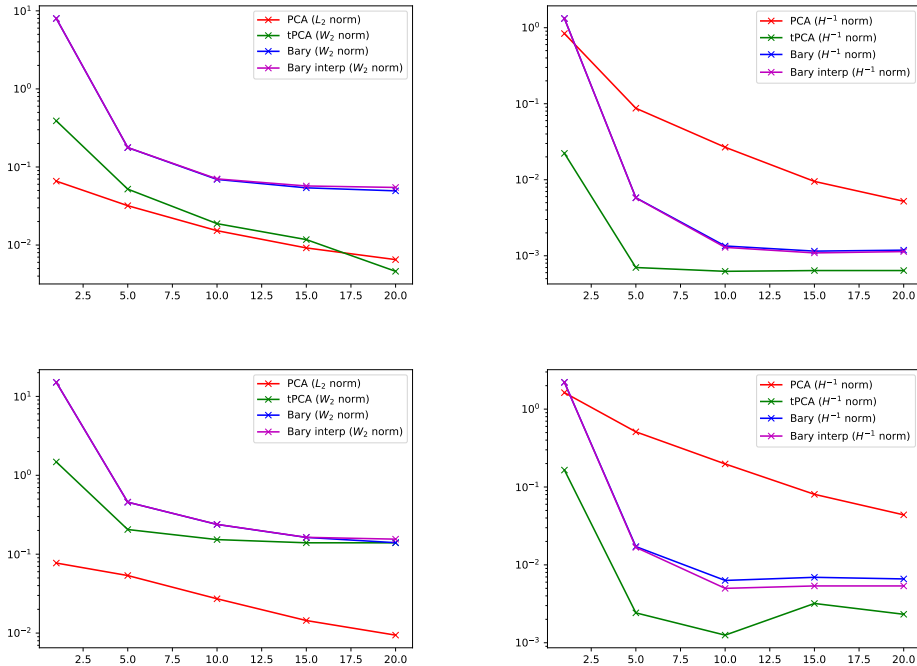


Figure 4: Errors on $\mathcal{M}_{\text{test}}$ for the CH equation. Top figures: average error. Bottom figures: worst case error. Left: natural norms. Right: H^{-1} norm.

6.4 Two-soliton solution of the Korteweg-de-Vries equation

The previous examples give solid numerical evidence that tPCA and our approach with barycenters are an efficient strategy to build reduced models of certain classes of transport dominated conservative PDEs. We finish the section on numerical results by presenting a PDE which poses certain challenges to the present methodology. This will serve as a transition that will lead us to the end of the paper where we present possible extensions to the present approach.

We consider a two soliton solution of the Korteweg-de-Vries equation (KdV) which, expressed in normalized units, reads for all $x \in \mathbb{R}$,

$$\partial_t u + 6u\partial_x u + \partial_x^3 u = 0.$$

The equation admits a general 2-soliton solution

$$u(x, t) = -2\partial_x^2 \log \det(I + A(x, t)), \quad (6.5)$$

where $A(x, t) \in \mathbb{R}^{2 \times 2}$ is the interaction matrix whose components $a_{i,j}$ are

$$a_{i,j}(x, t) = \frac{c_i c_j}{k_i + k_j} \exp((k_i + k_j)x - (k_i^3 + k_j^3)t), \quad 1 \leq i, j \leq 2.$$

For any $t > 0$, the total mass is equal to

$$\int_{\mathbb{R}} u(t, x) dx = 4(k_1 + k_2).$$

To illustrate the performance of our approach, we set

$$T = 2.5 \cdot 10^{-3}, \quad c_1 = 2, \quad c_2 = 3/2, \quad k_1 = 30 - k_2.$$

The parameter domain is

$$Z = \{(t, k_2) \in [0, 2.5 \cdot 10^{-3}] \times [16, 22]\}$$

It follows that the total mass is equal to 120 for all the parametric solutions.

Figure 5 gives the errors in average and worst case sense for a set of 500 test functions. The observed behavior resembles the one of our previous examples. However, note that this time the average errors are roughly of order 10 while they were of order 10^{-2} or 10^{-3} in the previous examples. A visual inspection of the reconstructed functions reveals that PCA is in this case not producing “worse-looking” reconstructions than the nonlinear methods (see Figure 9 of Appendix A). Two points can explain these observations: first, note that the exact solution does not present as sharp edges as in the other examples so this is playing in favor of PCA since it tends to produce oscillatory reconstructions. Second, in the present KdV evolution, we have two peakons of different masses propagating at different speeds. The fast peakon may overcome the slow one after a transition in which both peakons merge into a single one. Our strategy is based on a nonlinear mapping where translations can be treated simply but the mapping does not seem to be enough adapted to treat the case of fusion and separation of masses. This motivates to search for further nonlinear transformations to address this behavior. We outline some possibilities as well as further challenges in the next section.

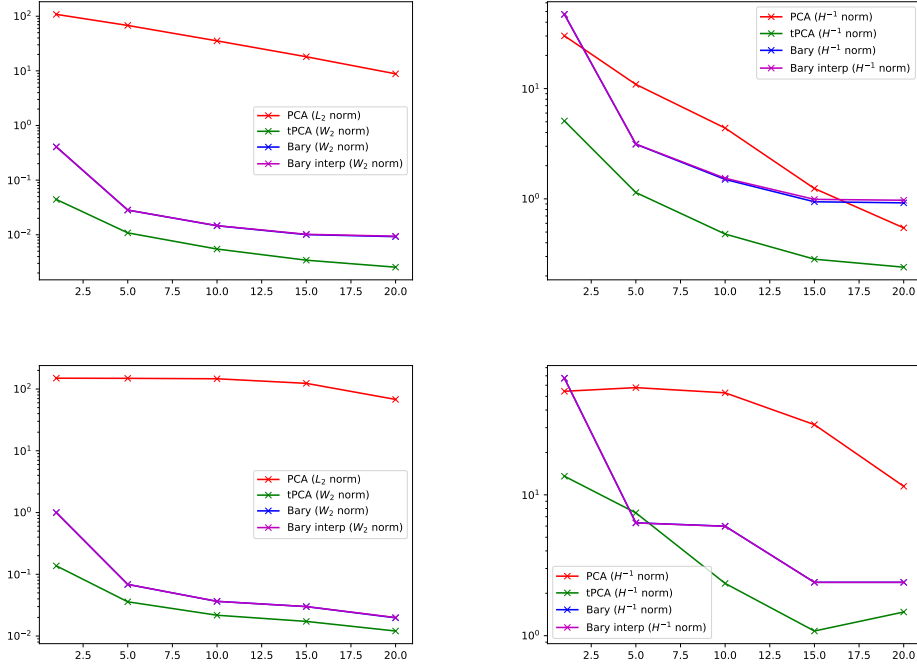


Figure 5: Errors on $\mathcal{M}_{\text{test}}$ for the KdV equation. Top figures: average error. Bottom figures: worst case error. Left: natural norms. Right: H^{-1} norm.

7 Conclusions and perspectives

In this work, we have shown how to exploit the geometry of some hyperbolic PDE in order to propose efficient reduced basis methods, one based on tangent PCA and one based on barycenters. These two methods are developed using the Wasserstein metric which captures the advection effects. There are multiple possible extensions to this work, among which stand the following:

- A first interesting theoretical question is the following: can the results of Section 3 on the decay of the Kolmogorov n -widths of the set \mathcal{T} be extended to more general transport equations, and under which assumptions?

- Can one obtain theoretical convergence rates of the greedy barycentric algorithm similar to the existing results on greedy algorithms for linear reduced bases [11, 44]?
- Can one reduce more complicated problems, i.e. defined on sets of dimension greater than one, or non-conservative problems, using one of the two presented algorithms? This seems to be the case at least for the barycentric greedy algorithm. Indeed, one can consider for instance the Hellinger-Kantorovich distance [?, 20], which appears to yield interesting approximation properties for problems where both transport and mass transfer phenomena occur. The computation of approximate barycenters of densities defined on spaces of dimension greater than one can be done using entropic regularization together with the Sinkhorn algorithm as proposed in [19] for instance.
- More generally, how to systematically select the best metric with respect to a given PDE and how to build non expensive surrogates of the exponential map? A promising direction to address these two issues seems to use machine learning algorithm to learn the metric for a given PDE [49], and then to learn the associated exponential map [24, 55].

We intend to address these issues in forthcoming works.

References

- [1] R. Abgrall, D. Amsallem, and R. Crisovan. Robust model reduction by L1-norm minimization and approximation via dictionaries: application to nonlinear hyperbolic problems. *Advanced Modeling and Simulation in Engineering Sciences*, 3(1):1, 2016.
- [2] B. M. Afkham and J. S. Hesthaven. Structure preserving model reduction of parametric hamiltonian systems. *SIAM Journal on Scientific Computing*, 39(6):A2616–A2644, 2017.
- [3] M. Agueh and G. Carlier. Barycenters in the Wasserstein Space. *SIAM Journal on Mathematical Analysis*, 43(2):904–924, 2011.
- [4] D. Amsallem and C. Farhat. Interpolation method for adapting reduced-order models and application to aeroelasticity. *AIAA journal*, 46(7):1803–1813, 2008.
- [5] D. Amsallem and B. Haasdonk. Pebl-rom: Projection-error based local reduced-order models. *Advanced Modeling and Simulation in Engineering Sciences*, 3(1):6, 2016.
- [6] D. Amsallem, M. J. Zahr, and C. Farhat. Nonlinear model order reduction based on local reduced-order bases. *International Journal for Numerical Methods in Engineering*, 92(10):891–916, 2012.
- [7] M. Barrault, Y. Maday, N. C. Nguyen, and A. T. Patera. An Empirical Interpolation Method: application to efficient reduced-basis discretization of partial differential equations. *C. R. Acad. Sci. Paris, Série I.*, 339:667–672, 2004.
- [8] P. Benner, A. Cohen, M. Ohlberger, and K. Willcox. *Model Reduction and Approximation: Theory and Algorithms*, volume 15. SIAM, 2017.
- [9] J. Bigot, R. Gouet, T. Klein, A. López, et al. Geodesic PCA in the Wasserstein space by Convex PCA. In *Annales de l’Institut Henri Poincaré, Probabilités et Statistiques*, volume 53, pages 1–26. Institut Henri Poincaré, 2017.
- [10] P. Binev, A. Cohen, W. Dahmen, R. DeVore, G. Petrova, and P. Wojtaszczyk. Convergence rates for greedy algorithms in reduced basis methods. *SIAM Journal on Mathematical Analysis*, 43(3):1457–1472, 2011.
- [11] P. Binev, A. Cohen, O. Mula, and J. Nichols. Greedy algorithms for optimal measurements selection in state estimation using reduced models. *SIAM/ASA Journal on Uncertainty Quantification*, 6(3):1101–1126, 2018.
- [12] A. Blanchet and P. Laurençot. The parabolic-parabolic keller-segel system with critical diffusion as a gradient flow in \mathbb{R}^d , $d \geq 3$. *Communications in Partial Differential Equations*, 38(4):658–686, 2013.
- [13] A. Bressan and M. Fonte. An optimal transportation metric for solutions of the Camassa-Holm equation. *Methods Appl Anal*, 12, 05 2005.
- [14] N. Cagniard, R. Crisovan, Y. Maday, and R. Abgrall. Model order reduction for hyperbolic problems: a new framework. 2017.

- [15] N. Cagniard, Y. Maday, and B. Stamm. Model order reduction for problems with large convection effects. In *Contributions to Partial Differential Equations and Applications*, pages 131–150. Springer, 2019.
- [16] K. Carlberg. Adaptive h-refinement for reduced-order models. *International Journal for Numerical Methods in Engineering*, 102(5):1192–1210, 2015.
- [17] J. A. Carrillo, K. Grunert, and H. Holden. A lipschitz metric for the hunter–saxton equation. *Communications in Partial Differential Equations*, 44(4):309–334, 2019.
- [18] E. Cazelles, V. Seguy, J. Bigot, M. Cuturi, and N. Papadakis. Log-PCA versus Geodesic PCA of histograms in the Wasserstein space. *arXiv preprint arXiv:1708.08143*, 2017.
- [19] L. Chizat, G. Peyré, B. Schmitzer, and F.-X. Vialard. Scaling algorithms for unbalanced transport problems. *Mathematics of Computation*, 87:2563–2609, 2018.
- [20] L. Chizat, B. Schmitzer, G. Peyré, and F.-X. Vialard. An interpolating distance between optimal transport and Fischer-rao. *Foundations of Computational Mathematics*, 18(1):1–44, 2018.
- [21] A. Cohen and R. DeVore. Kolmogorov widths under holomorphic mappings. *IMA Journal of Numerical Analysis*, 36(1):1–12, 2016.
- [22] A. Cohen, R. DeVore, and C. Schwab. Convergence rates of best n-term galerkin approximations for a class of elliptic spdes. *Foundations of Computational Mathematics*, 10(6):615–646, 2010.
- [23] A. Cohen, R. DeVore, and C. Schwab. Analytic regularity and polynomial approximation of parametric and stochastic elliptic PDE’s. *Analysis and Applications*, 09(01):11–47, 2011.
- [24] Z. Ding, G. Fleishman, X. Yang, P. Thompson, R. Kwitt, and M. Niethammer. Fast Predictive Simple Geodesic Regression. In Cardoso M. et al., editor, *Lecture Notes in Computer Science: 14th International Conference*, volume 10553. Springer, Cham, 2017.
- [25] F. Feppon and P. F. J. Lermusiaux. A geometric approach to dynamical model order reduction. *SIAM Journal on Matrix Analysis and Applications*, 39(1):510–538, 2018.
- [26] P. Thomas Fletcher, Conglin Lu, Stephen M. Pizer, and Sarang C. Joshi. Principal geodesic analysis for the study of nonlinear statistics of shape. *IEEE Transactions on Medical Imaging*, 23:995–1005, 2004.
- [27] J. P. Gazeau and P. Winternitz. Symmetries of variable coefficient korteweg–de vries equations. *Journal of mathematical physics*, 33(12):4087–4102, 1992.
- [28] L. Giacomelli and F. Otto. Variational formulation for the lubrication approximation of the hele-shaw flow. *Calculus of Variations and Partial Differential Equations*, 13(3):377–403, 2001.
- [29] U. Gianazza, G. Savaré, and G. Toscani. The wasserstein gradient flow of the fisher information and the quantum drift-diffusion equation. *Archive for rational mechanics and analysis*, 194(1):133–220, 2009.
- [30] F. J Gonzalez and M. Balajewicz. Learning low-dimensional feature dynamics using deep convolutional recurrent autoencoders. *arXiv preprint arXiv:1808.01346*, 2018.
- [31] C. Greif and K. Urban. Decay of the kolmogorov n-width for wave problems. *Applied Mathematics Letters*, 96:216–222, 2019.
- [32] M.A. Grepl, Y. Maday, N.C. Nguyen, and A.T. Patera. Efficient reduced-basis treatment of nonaffine and nonlinear partial differential equations. *ESAIM, Math. Model. Numer. Anal.*, 41(3):575–605, 2007.
- [33] J. S. Hesthaven and C. Pagliantini. Structure-preserving reduced basis methods for hamiltonian systems with a nonlinear poisson structure. Technical report, 2018.
- [34] J. S. Hesthaven, G. Rozza, and B. Stamm. Certified Reduced Basis Methods for Parametrized Partial Differential Equations. *SpringerBriefs in Mathematics*, 2015.
- [35] S. Huckemann, T. Hotz, and A. Munk. Intrinsic shape analysis: Geodesic pca for riemannian manifolds modulo isometric lie group actions. *Statistica Sinica*, 20(1):1–58, 2010.
- [36] A. Iollo and D. Lombardi. Advection modes by optimal mass transfer. *Physical Review E*, 89(2):022923, 2014.
- [37] R. Jordan, D. Kinderlehrer, and F. Otto. The variational formulation of the fokker–planck equation. *SIAM journal on mathematical analysis*, 29(1):1–17, 1998.
- [38] B. N Khoromskij and C. Schwab. Tensor-structured galerkin approximation of parametric and stochastic elliptic pdes. *SIAM Journal on Scientific Computing*, 33(1):364–385, 2011.

- [39] O. Koch and C. Lubich. Dynamical low-rank approximation. *SIAM Journal on Matrix Analysis and Applications*, 29(2):434–454, 2007.
- [40] O. Koch and C. Lubich. Dynamical tensor approximation. *SIAM Journal on Matrix Analysis and Applications*, 31(5):2360–2375, 2010.
- [41] K. Lee and K. Carlberg. Model reduction of dynamical systems on nonlinear manifolds using deep convolutional autoencoders. *arXiv preprint arXiv:1812.08373*, 2018.
- [42] Y. Maday, A. Manzoni, and A. Quarteroni. An online intrinsic stabilization strategy for the reduced basis approximation of parametrized advection-dominated problems. *Comptes Rendus Mathematique*, 354(12):1188–1194, 2016.
- [43] Y. Maday and O. Mula. A Generalized Empirical Interpolation Method: application of reduced basis techniques to data assimilation. In Franco Brezzi, Piero Colli Franzone, Ugo Gianazza, and Gianni Gilardi, editors, *Analysis and Numerics of Partial Differential Equations*, volume 4 of *Springer INdAM Series*, pages 221–235. Springer Milan, 2013.
- [44] Y. Maday, O. Mula, and G. Turinici. Convergence analysis of the generalized empirical interpolation method. *SIAM Journal on Numerical Analysis*, 54(3):1713–1731, 2016.
- [45] R. Mosquera, A. Hamdouni, A. El Hamiidi, and C. Allery. POD basis interpolation via Inverse Distance Weighting on Grassmann manifolds. *Discrete & Continuous Dynamical Systems - S*, 12(1937-1632):1743, 2019.
- [46] S. Mowlavi and T. P. Sapsis. Model order reduction for stochastic dynamical systems with continuous symmetries. *SIAM Journal on Scientific Computing*, 40(3):A1669–A1695, 2018.
- [47] E. Musharbash, F. Nobile, and T. Zhou. Error analysis of the dynamically orthogonal approximation of time dependent random pdes. *SIAM Journal on Scientific Computing*, 37(2):A776–A810, 2015.
- [48] N. J. Nair and M. Balajewicz. Transported snapshot model order reduction approach for parametric, steady-state fluid flows containing parameter-dependent shocks. *International Journal for Numerical Methods in Engineering*, 2018.
- [49] M. Niethammer, R. Kwitt, and F.-X. Vialard. Metric learning for image registration. In *Proceedings of the IEEE Conference on Computer Vision and Pattern Recognition*, pages 8463–8472, 2019.
- [50] M. Ohlberger and S. Rave. Nonlinear reduced basis approximation of parameterized evolution equations via the method of freezing. *Comptes Rendus Mathematique*, 351(23-24):901–906, 2013.
- [51] F. Otto. The geometry of dissipative evolution equations: the porous medium equation. 2001.
- [52] B. Peherstorfer, D. Butnaru, K. Willcox, and H.-J. Bungartz. Localized discrete empirical interpolation method. *SIAM Journal on Scientific Computing*, 36(1):A168–A192, 2014.
- [53] X. Pennec. Barycentric subspace analysis on manifolds. *The Annals of Statistics*, 46(6A):2711–2746, 2018.
- [54] A. Quarteroni, A. Manzoni, and F. Negri. *Reduced basis methods for partial differential equations: an introduction*, volume 92. Springer, 2015.
- [55] Z. Shen, F.-X. Vialard, and M. Niethammer. Region-specific Diffeomorphic Metric Mapping. *NeurIPS*, page arXiv:1906.00139, Dec 2019.
- [56] S. Sommer, F. Lauze, and M. Nielsen. Optimization over geodesics for exact principal geodesic analysis. *Advances in Computational Mathematics*, 40(2):283–313, Apr 2014.
- [57] D. Torlo, F. Ballarin, and G. Rozza. Stabilized weighted reduced basis methods for parametrized advection dominated problems with random inputs. *SIAM/ASA Journal on Uncertainty Quantification*, 6(4):1475–1502, 2018.
- [58] C. Villani. *Topics in optimal transportation*. Number 58. American Mathematical Soc., 2003.
- [59] G. Welper. Transformed snapshot interpolation. *arXiv preprint arXiv:1505.01227*, 2015.
- [60] G. Welper. h and hp -adaptive interpolation by transformed snapshots for parametric and stochastic hyperbolic pdes. *arXiv preprint arXiv:1710.11481*, 2017.
- [61] J. Zinsl and D. Matthes. Exponential convergence to equilibrium in a coupled gradient flow system modeling chemotaxis. *Analysis & PDE*, 8(2):425–466, 2015.

A Reconstruction plots

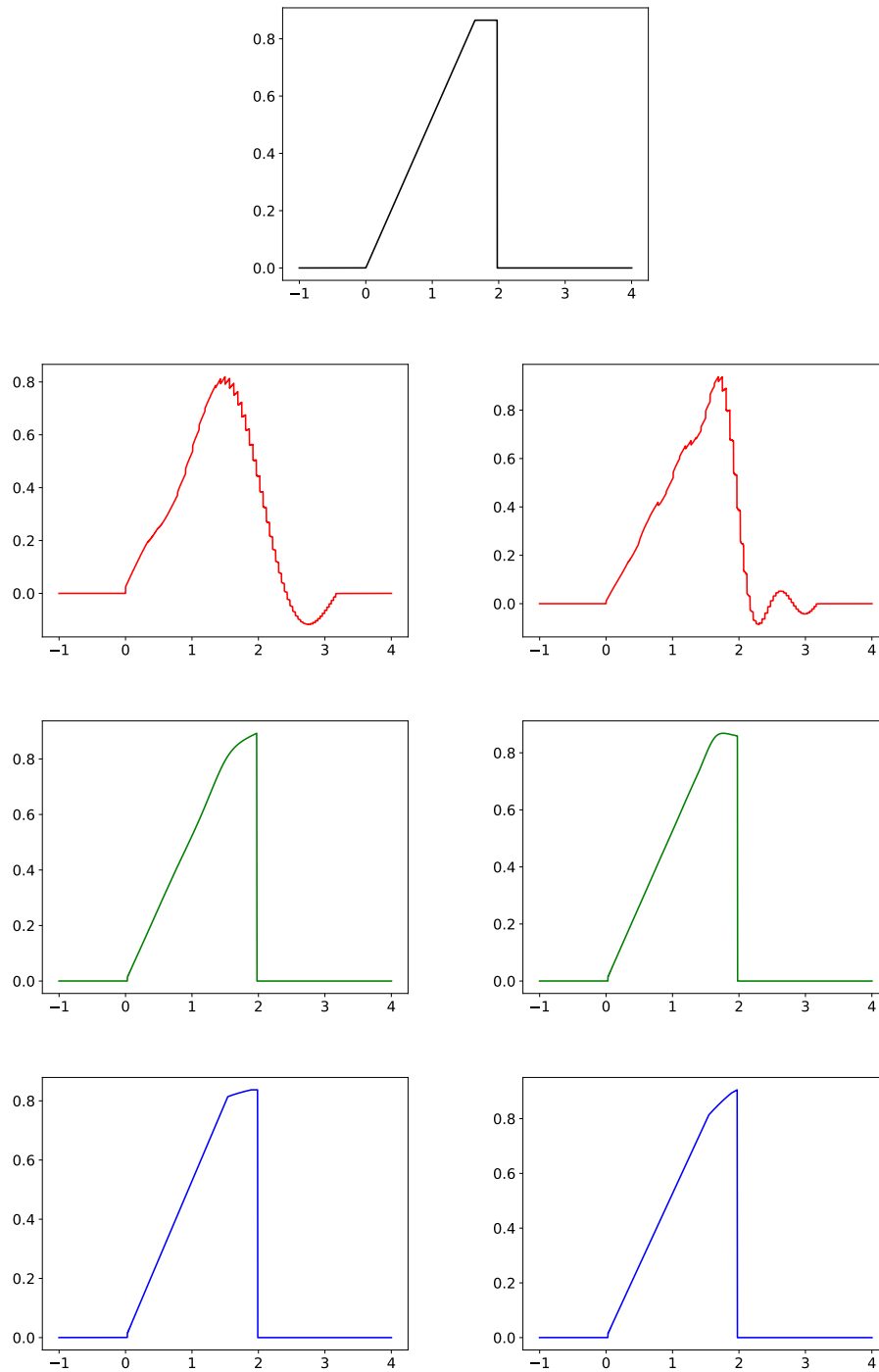


Figure 6: Burgers equation: Reconstruction of a function with $n = 5$ (left) and $n = 10$ (right). Black: exact function. Red: PCA. Green: tPCA. Blue: Barycenter.

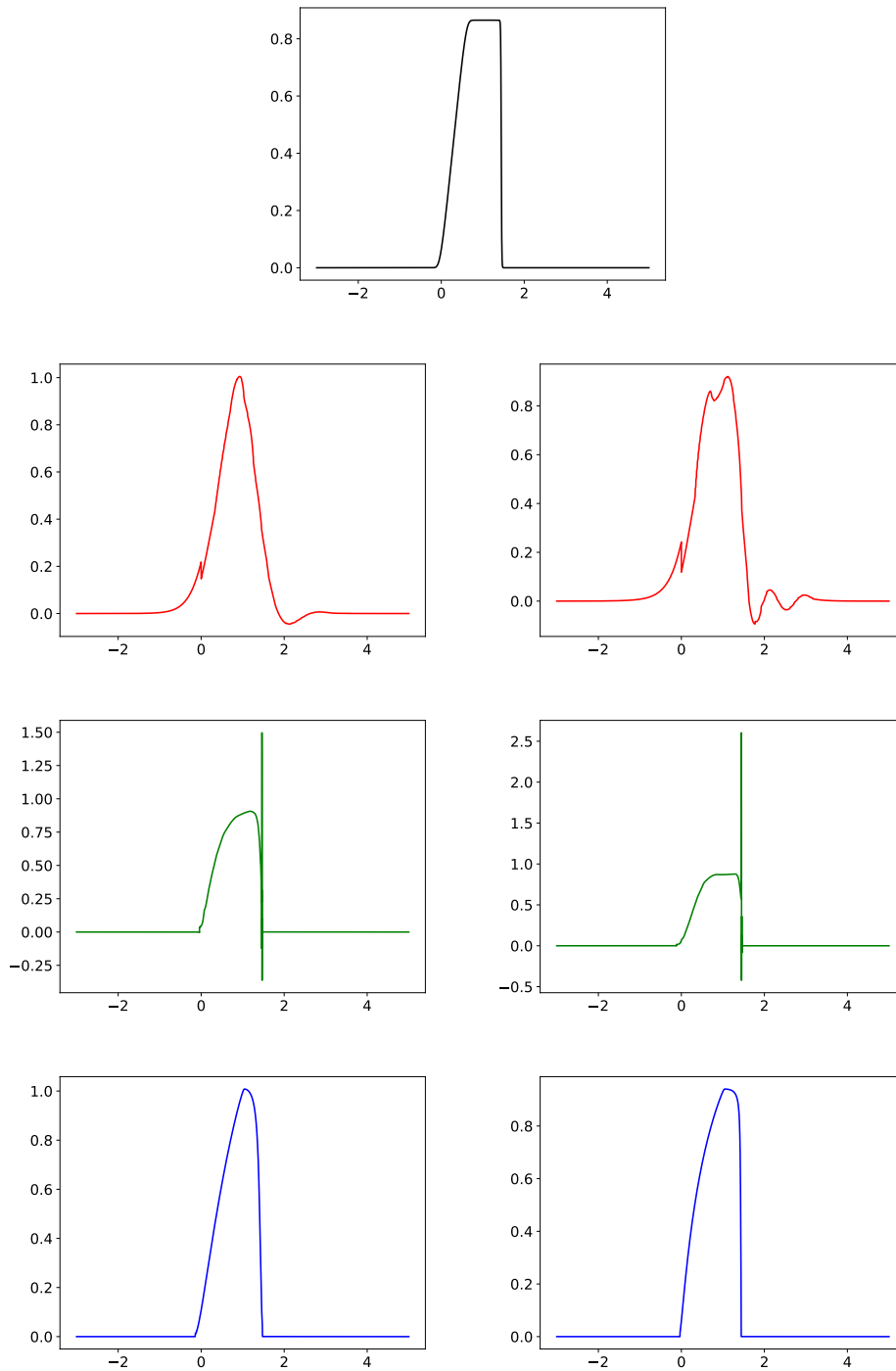


Figure 7: ViscousBurgers equation: Reconstruction of a function with $n = 5$ (left) and $n = 10$ (right). Black: exact function. Red: PCA. Green: tPCA. Blue: Barycenter.

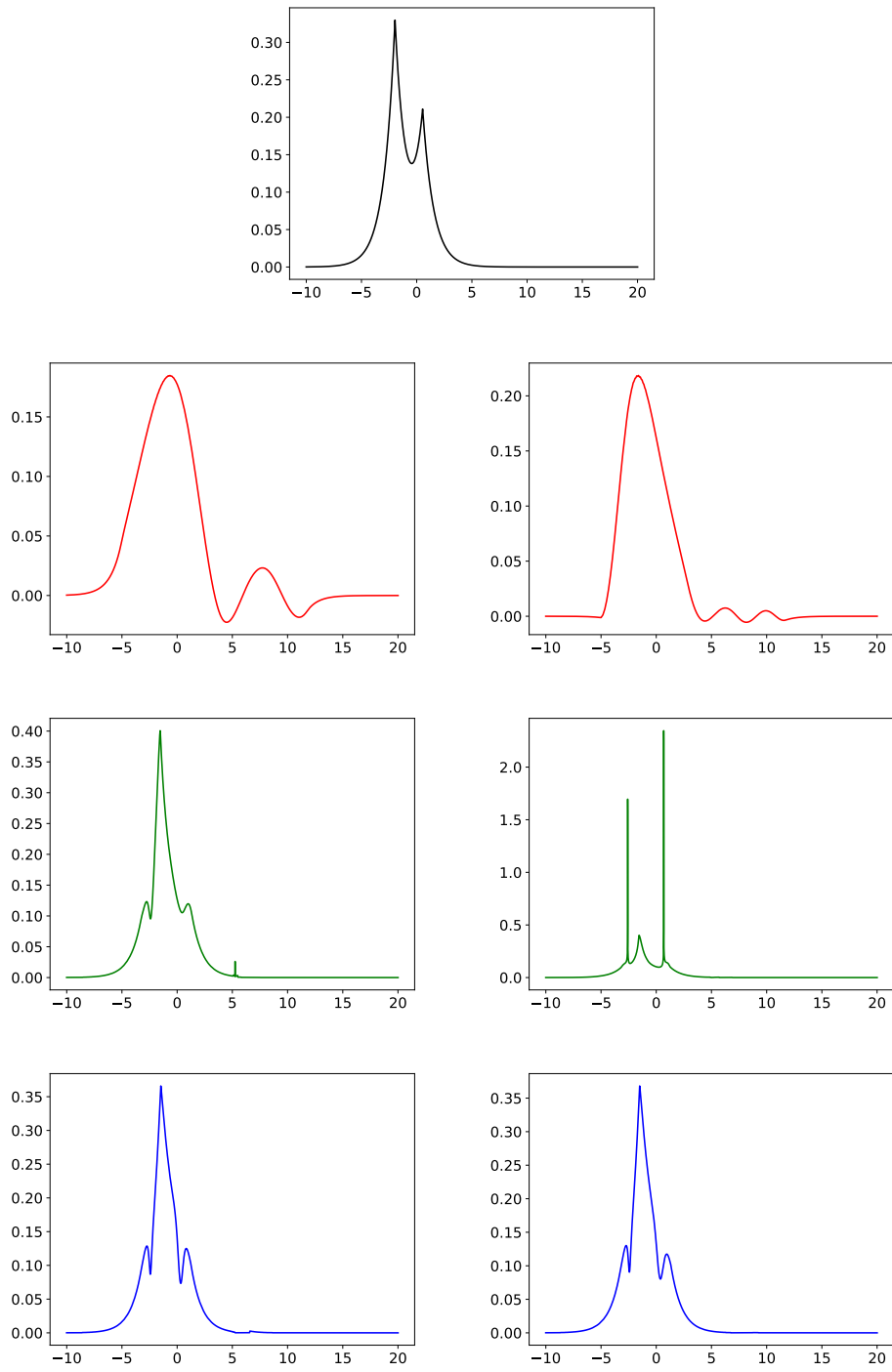


Figure 8: CH equation: Reconstruction of a function with $n = 5$ (left) and $n = 10$ (right). Black: exact function. Red: PCA. Green: tPCA. Blue: Barycenter.

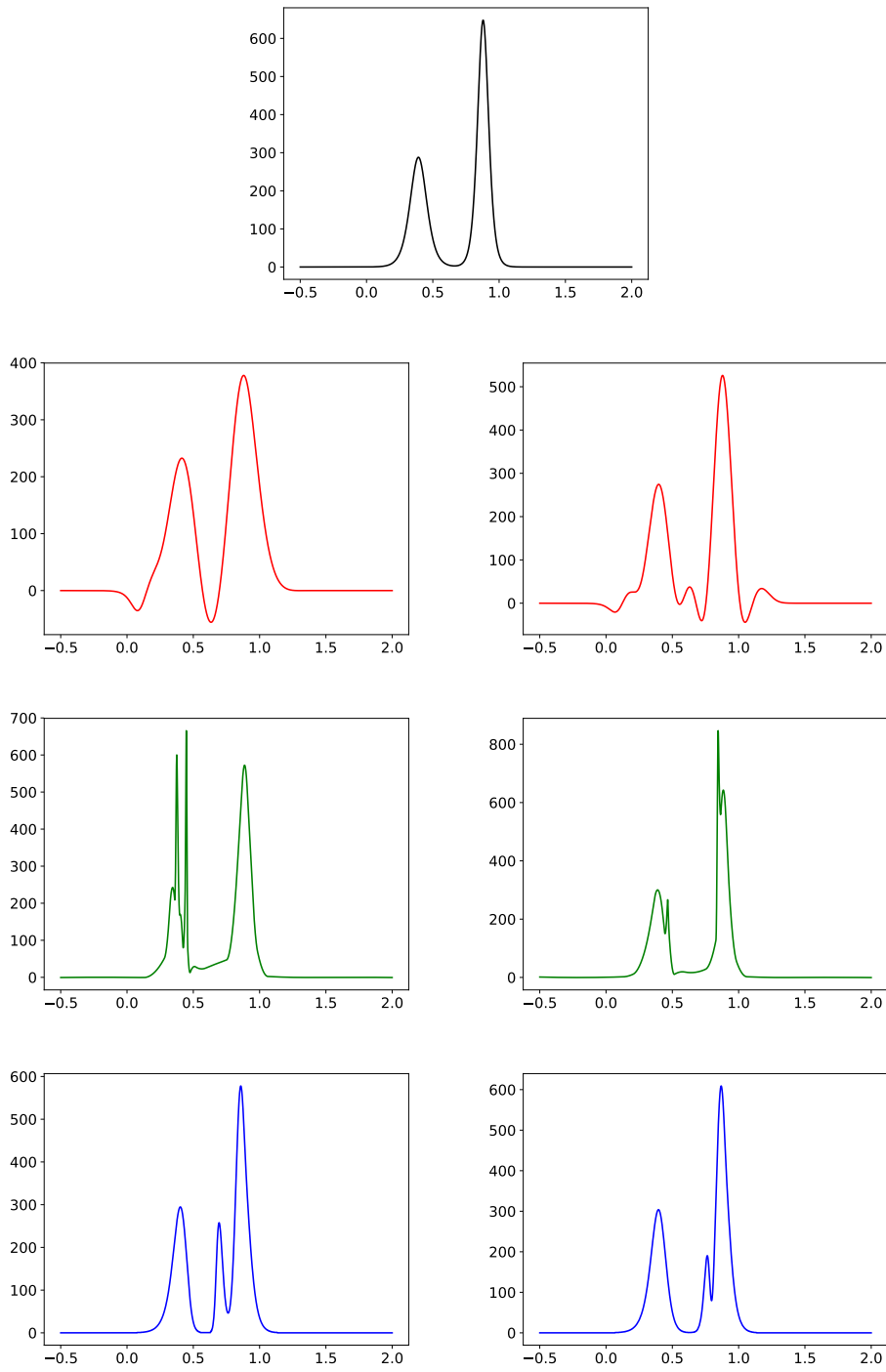


Figure 9: KdV equation: Reconstruction of a function with $n = 5$ (left) and $n = 10$ (right). Black: exact function. Red: PCA. Green: tPCA. Blue: Barycenter.